ACS APPLIED MATERIALS & INTERFACES

www.acsami.org Review

Review of Vertical Graphene and its Applications

Wei Zheng, Xin Zhao, and Wenjie Fu*

Cite This: *ACS Appl. Mater. Interfaces* 2021, 13, 9561–9579 Read Online

ACCESS | Metrics & More | Article Recommendations

ABSTRACT: Vertical graphene (VG) is a thin-film complex material featuring hierarchical microstructures: graphene-containing carbon nanosheets growing vertically on its deposition substrate, few-layer graphene basal layers, and chemically active atomistic defect sites and edges. Thanks to the fundamental characteristics of graphene materials, e.g. excellent electrical conductivity, thermal conductivity, chemical stability, and large specific surface area, VG materials have been successfully implemented into various niche applications which are strongly associated with their unique morphology. The microstructure of VG materials can be tuned by modifying growth methods and the parameters of growth processes. Multiple growth processes have been developed to address faster, safer, and mass production methods of VG materials, as well as accommodating various applications. VG's successful applications include field emission, supercapacitors, fuel cells, batteries, gas sensors, biochemical sensors, electrochemical analysis, strain sensors, wearable electronics, photo trapping, terahertz emission, etc. Research topics on VG have been more diversified in recent years, indicating extensive attention from the research community and great commercial value. In this review article, VG's morphology is briefly reviewed, and then various growth processes are discussed from the perspective of plasma science. After that, the most recent progress in its applications and related sciences and technologies are discussed.

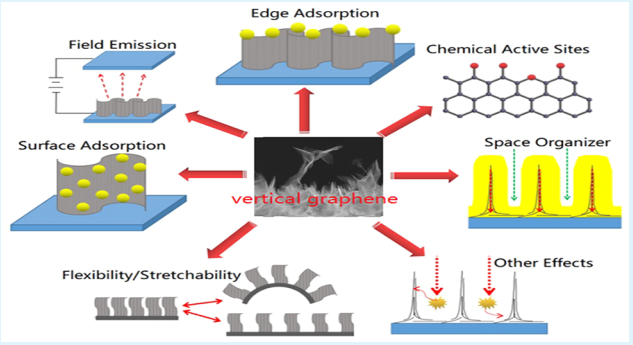

KEYWORDS: *vertical graphene, carbon nanosheets, carbon nanowall, graphene edges, graphene defects*

1. INTRODUCTION

Research on graphene has been very extensive during the last two decades, especially after the Nobel Prize in Physics in 2010 was awarded "for groundbreaking experiments regarding the two-dimensional material graphene." While research on graphene's basic physical and chemical properties is plethoric, scientists are committed to finding its irreplaceable applications in order to develop commercial value. Such applications should have advantages over its competitors in certain aspects. In this review article, we focus on one unique class of graphene-based complex material with a variety of potential applications based on its special features. This thin film material is named hereby as vertical graphene (VG) because it is primarily composed of few-layer graphene-containing carbon nanosheets growing vertically on its deposition substrate. The earliest report on this material can be traced back to 1997, when Ando found petal-like "carbon roses" during the fabrication of carbon nanotubes.[1] Multiple names, such as vertical graphene nanosheet, vertically oriented graphene, carbon nanowalls, carbon nanoflakes, carbon nanosheets, edge-oriented graphene, vertically aligned few-layered graphene nanoflakes, free-standing subnanometer graphite sheets, vertically stacked graphene networks, vertically aligned graphene nanosheet arrays, etc., have been historically used to refer to this class of materials by different research groups.[2,3]

Figure 1a depicts VG structure, with a standard name and measure for each part to be used in this article. The morphology of VG is mainly composed of three components, which are edges of few-layer graphene, vertically free-standing few-layer graphene-containing carbon nanosheets (CNSs), and few-layer graphene-containing basal layers (basal layers). As a result of the few-layer graphene constitution, VG has many of the fundamental characteristics of graphene materials, for example, high electrical conductivity, thermal conductivity, chemical stability, large specific surface area, chemically active edges and defects, and the highest ratio of edge atoms of any carbon allotrope. VG contains a large number of sharp, exposed, and vertically pointed edges (Figure 1b), which is favorable for field emission applications (Figure 1c). Furthermore, because the atoms at graphene edges have

Received: October 26, 2020
Accepted: February 12, 2021
Published: February 22, 2021

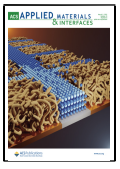

https://dx.doi.org/10.1021/acsami.0c19188
ACS Appl. Mater. Interfaces 2021, 13, 9561–9579

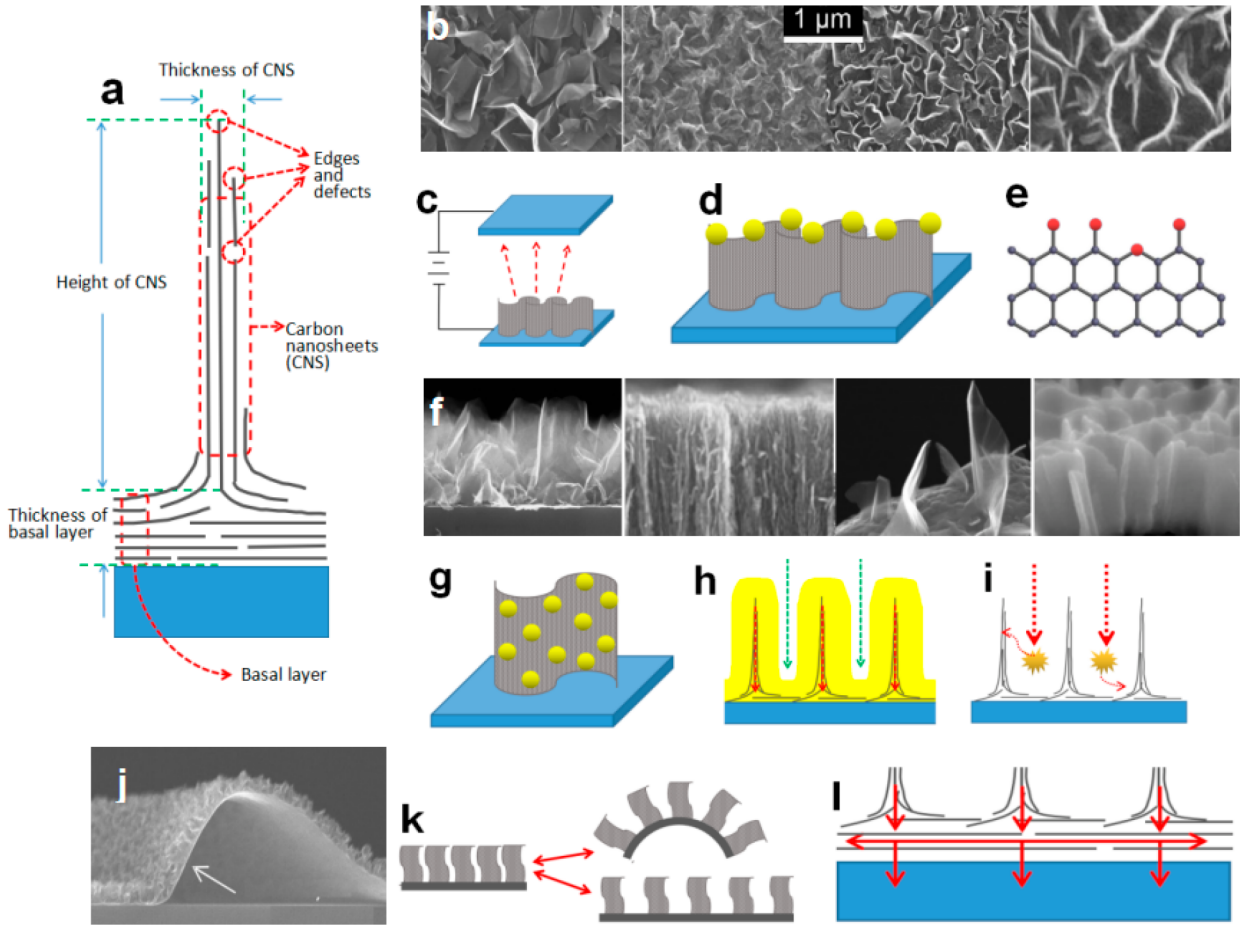

Figure 1. (a) Illustration of the structure of vertical graphene (VG). (b) SEM images showing various morphologies of VG edges [Reprinted with permission from refs 4 (Copyright 2006 Mingyao Zhu) and 102 (Copyright 2014 Elsevier)]. (c) VG edges in application of field emission, (d) adsorption of functional materials, and (e) forming bonds with dopant atoms. (f) SEM images showing various morphologies of carbon nanosheets (CNS) [Reprinted with permission from refs 4 (Copyright 2006 Mingyao Zhu), 8 (Copyright 2014 Elsevier), 78 (Copyright 2010 AAAS), and 102 (Copyright 2002 Wiley-VCH)]. (g) Illustration of VG CNS as nanoparticle carrier, (h) spacial organizer, electrical charge conductor, and (i) photo trap. (j) SEM image showing basal layer of VG [Reprinted with permission from ref 132. Copyright 2015 SpringerOpen]. (k) Illustration of basal layer playing important roles in stretch/flexible electrodes and (l) in-plane thermal and electrical current distribution.

special chemical reactivity, the edges provide sites to adsorb functional materials and dopants (Figure 1d,e). A CNS usually has a growth height ranging from a couple hundreds of nanometers to several tens of micrometers, its average sheet thickness can be as thin as a couple of nanometers, and its shape can be straight, curved, folded, and corrugated (Figure 1f). A CNS provides most of the surface area of VG, which is about 1000 m^2/g.[4] Electrostatic double-layer capacitors (EDLCs) and uniform carrying of nanoparticles of functional material on CNSs are direct applications utilizing the large surface area (Figure 1g). In addition to the large surface area, defects on CNSs are favorable to bind various dopants and functional materials and facilitate the transfer of charges. The CNS morphology can also function as a space organizer in nanoscale. In the case of mass loading of functional materials, CNSs prevent aggregation of these condensed materials. The open structure between CNSs provides passages for the bottoms of CNSs to be accessible by analytic or functional chemicals. Moreover, the CNS itself works as a highway for the electric charges transferring from the top to the bottom. All of the above factors make VG an efficient electric charge carrying and mechanical supporting structure (Figure 1h). The CNS morphology also makes VG a good photon trapper (Figure 1i), which has application in photothermal heaters and terahertz (THz) emission. The basal layer (Figure 1j) has been observed for years, but its importance has not been applied and elucidated until recently. It plays the most important role in the flexibility and stretchability of VG composite electrodes (Figure 1k). As an outstanding conductor for both electrical charges and heat, the basal layer renders a uniform in-plane heat and electrical current distribution. Furthermore, the in situ crystal nucleation and grain growth of VG reduces the contact resistance between the basal layer and the substrate as an electrical current collector (Figure 1k). The basal layer only exists in VG materials being prepared by the "bottom-up" crystal material growth process. Other graphene materials with a similar "crumpled-nanosheets" appearance but prepared by other "top-down" materials processing methods will not have such a unique basal layer structure by nature; therefore, they are excluded from this review article.

The research into VG was initially focused on reporting its fascinating nanostructure, growth methods, growth mechanism, and material characterization. For example, microwave plasma enhanced chemical vapor deposition (MPCVD),[5,6] and radio frequency (RF) inductively coupled plasma enhanced chemical vapor deposition (ICP-PECVD),[7] with different

https://dx.doi.org/10.1021/acsami.0c19188
ACS Appl. Mater. Interfaces 2021, 13, 9561−9579

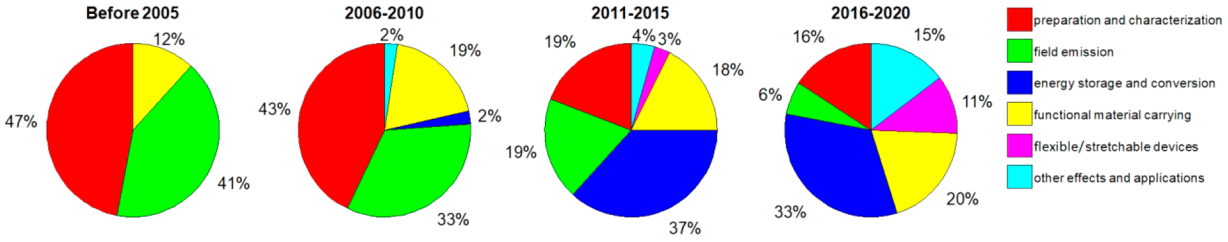

Figure 2. Major topics of research in VG over the past two decades.

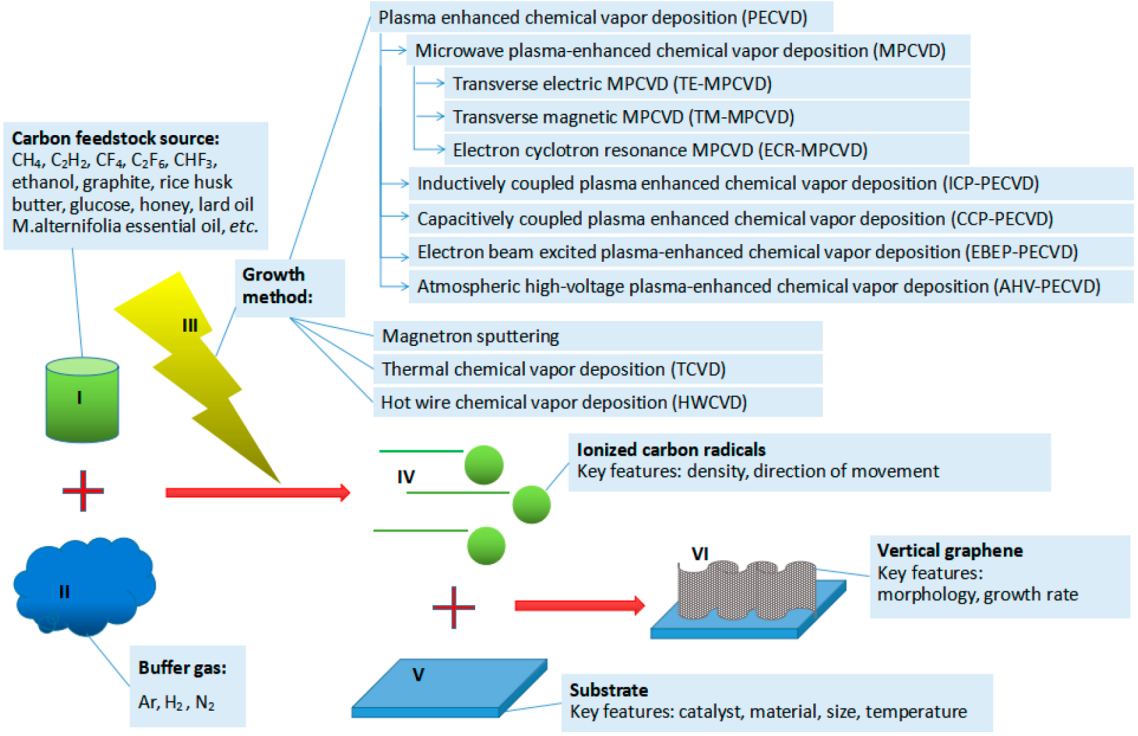

Figure 3. Major parameters in the VG growth process.

precursors (sources of carbon feedstock) and other parameters, are the growth methods being intensively studied. A major task is to control the VG morphology via manipulating the process parameters. Note that the pristine VG is hydrophobic, thus unfavorable to many applications. Therefore, postgrowth treatments are often applied to make VG hydrophilic. These treatments will be elaborated in the following sections. In section 2, we will briefly review the growth methods, as well as features of various plasma sources. We will also disclose how growth methods affect the morphology of VG in a general way. Since the discovery of VG, the community has never stopped finding new applications. Field emission was an obvious choice at the beginning. Pioneering research groups have reported VG application in field emission,[6,7] and this topic contributed more than one-third of the publications before 2010 according to our statistics. Although a VG field emitter has not been commercialized yet, related research has triggered a deeper exploration of VG morphology, especially controlling of morphology via either in situ and postgrowth treatment. We will elaborate these efforts and summarize the interesting features in section 3. Composite materials composed of VG as a supporting structure and other materials as functional materials have been studied as early as in 2002.[8] A large percentage of the publications in the previous two decades were related to research in this direction. Sorts of functional materials, e.g. metal nanoparticles, chemical compounds, enzymes, DNAs, and even live cells, have been studied. A variety of deposition methods were applied and each had different effects combined with the VG morphology. In section 4, we will summarize the deposition methods, the resulting morphology of the composite materials, as well as the benefits brought by them, providing guidance for wider applications in the future. Multiple flexible/stretchable electronic devices containing VG electrodes have been reported since 2015. VG's basal layer is the key factor for high performance flexible/stretchable electrodes. This application has a great commercialization potential due to the emerging market of flexible/stretchable and wearable devices. We will elaborate the mechanism and interesting findings in section 5. Research into VG's applications in energy storage and conversion has been paid special attention for the past ten years and was summarized elaborately by Zhang.[9] With different perspectives, in section 6 we will focus on the problems encountered and the approaches of scientists to solve the problems. Some interesting results of the most recent research are included. The diversity of research and applications of VGs has increased dramatically since 2015. We will mention the interesting applications based on physical, electronic, electromagnetic,

https://dx.doi.org/10.1021/acsami.0c19188
ACS Appl. Mater. Interfaces 2021, 13, 9561−9579

electrochemical, optical, and thermal properties of VG in section 7. Figure 2 shows rough statistics which provide a basic idea of the major topics of researches in VG covered by this review article.

2. GROWTH PROCESS

An interesting fact is that VG was discovered unexpectedly. Other carbon materials, e.g. diamond, carbon nanotubes (CNTs), or graphene, are supposed to grow, but it turns out that VG was actually created.[1] To grow VG, multiple approaches have been demonstrated successfully. Published works have reported detailed information on the growth processes. We will summarize some important trends out of an emerging number of growth processes being reported, as well as some qualitative analysis and comparisons. In the literature, "crystal growth", "synthesis", "preparation", "fabrication", and "thin-film deposition" are all used to refer to this process. We mainly use "growth" hereby, taking into consideration that VG is a thin film and single component material, in line with the established knowledge framework from international thin-film materials science societies.

We will focus on the bottom-up growth processes of VG, which is a term of material science referring to any material process originating from self-organizing crystal grain growth of carbon species radicals, in contrast to top-down processes that mechanically engineering the structure of already existed carbon bulk materials from mineral graphite flakes. In such bottom-up processes, the carbon feedstock (or precursor) source (I), buffer gas (II), growth method (III), ionized carbon radical (IV), growth substrate (V), and obtained VG (VI) are the major parameters (Figure 3) that researchers work on. Historically, using methane (CH_4) as a carbon gaseous source (or precursor), low pressure plasma enhanced chemical vapor deposition (PECVD) as the growth method, and heated substrates to grow VG is a traditional recipe. Researchers gradually developed novel recipes using different carbon sources and different growth methods. For example, Seo reported a synthesis process using honey as the solid carbon source, a mixture of Ar and H_2 as a buffer gas, and inductively coupled plasma enhanced chemical vapor deposition (ICP-PECVD) as both a growth method and heating source for the substrate.[10] Bo reported fast synthesis of VG with atmospheric high voltage PECVD (AHV-PECVD).[11] A furnace with temperatures of 800−900 °C that can thermally crack CH_4 into ionized carbon radicals for VG growth was reported by Guo. This is called thermal chemical vapor deposition (TCVD).[12] Zheng reported a thermal decomposition method using an SiC substrate with 1600 °C thermal treatment.[13] Magnetron sputtering and thermal hot wire chemical vapor deposition (HWCVD) have also been reported.[14,15]

Motion direction of charged particles and plasma density are two critical parameters of plasma that affect VG's growth. More specifically, microwave plasma-enhanced chemical vapor deposition (MPCVD),[5,6] ICP-PECVD,[7] capacitively coupled plasma enhanced chemical vapor deposition (CCP-PECVD),[16,17] electron beam excited plasma-enhanced chemical vapor deposition (EBEP-PECVD),[18] and AHV-PECVD are types of PECVD having been used to grow VG. MPCVD was adopted in the earliest reports of VG and are commonly used in diamond and CNS synthesis. There are three kinds of microwave plasma, transverse electric (TE) mode,[19] transverse magnetic (TM) mode,[20] and electron cyclotron resonance (ECR) mode,[21] depending on microwave propagation characteristics. In the TE mode, the electric field is only in the transverse direction (orthogonal to the direction of propagation) and drives the charged particles to move in a direction perpendicular to the substrate plane in a normal configuration. In the TM mode, the magnetic field is in the transverse direction, and the electric field is only in the direction of propagation. The TM mode causes in-plane (substrate plane) motion of the electrons and ionized carbon radicals on the microwave time scale. In ECR mode, the electron transport properties become tensors and functions of a static magnetic flux density, which leads to a three-component vector motion of electrons and ionized carbon radicals. Inductively coupled plasma (ICP) is generated from radio frequency (RF) magnetic fields induced by a water- or air-cooled copper coil. ICP mode can be used for a wide range of carbon sources. The frequency is usually in tens of kHz to tens of MHz. A frequency of 13.56 MHz RF is mostly used in industrial and scientific applications. In ICP mode, ionized carbon radicals move in the same direction with the current in the coil. There are typically two approaches to this type of plasma generation, planar ICP and tube/cylinder ICP, each having a distinct basic structure. The planar ICP is a flat coil with a quartz or ceramic window,[22] and the tube/cylinder ICP has a quartz or ceramic tube with coils around it.[23] For either planar ICP or tube/cylinder ICP, in common practice, the movement of ionized carbon radicals is parallel to the plane of substrate. Capacitively coupled plasma (CCP) is a plasma generated between two parallel plates of a capacitor while gases are fed into the chamber. RF power or DC voltage is applied to one of the plates while the other is grounded or floated. CCP is sometimes combined with other plasma techniques, e.g. inductively coupled plasma (ICP) and surface-wave-sustained plasma (SWP) to synthesis VG, which enhances the growth rate but largely increases the overall complexity.[16,17] CCP drives the ionized carbon radicals to move perpendicularly to the substrate plane in the configurations which have been reported. In AHV-PECVD, the ionized carbon radicals are driven by the high voltage field to move in a direction perpendicular to the substrate surface, but it is hard to grow VG on a large size substrate. EBEP-PECVD is a hybrid system, using DC discharge followed by electron extraction and acceleration as plasma source. The DC discharge plasma is sustained by electrons emitted from a cathode made of a LaB_6 disk. The electron beam is extracted from the DC discharge plasma and is accelerated by a pair of multihole grids into the EBEP region. The electrons and ionized carbon radicals move mainly in the direction perpendicular to the substrate with the constraint of the applied electric field. For other synthesis methods, the ionized carbon radicals move mainly perpendicularly to the substrate plane in magnetron sputtering and in a pretty random way in TCVD and HWCVD.

The plasma density is related to the background pressure being excited. The gas concentration of the atmospheric pressure environment is much higher than that of low pressure environments in the vacuum system, so the plasma density of atmospheric high-voltage plasma is much higher than that of the low-pressure plasma. Based on plasma physics, the higher the frequency of the electromagnetic field, the higher the plasma density. The density of microwave plasma in a fully excited state is higher than that of RF ICP. An example is reported by Chuang et al., in which an extreme VG growth rate is obtained in a TM-MPCVD system which is plasma generated at 10 Torr pressure.[20] However, generally speaking

https://dx.doi.org/10.1021/acsami.0c19188
ACS Appl. Mater. Interfaces 2021, 13, 9561−9579

Table 1. Methods to Enhance Field Emission Performance

VG growth process and parameters	treatment	observations of enhancement	ref
RF ICP-PECVD CH_4:H_2 = 4:6 600 nm high, 1 nm thick	3 monolayers (∼1 nm thick) of molybdenum were deposited on VG by magnetron sputtering, then Mo_2C formed by heating to 200 °C at 10^{-8} Torr	greater than a factor of 100 increase in current and greater than 2 V/μm decrease in threshold, in comparison to pristine VG emitter; enhancement factor ∼ 530	28
RF ICP-PECVD CH_4:H_2 = 4:6 1000 nm high, 1−2 nm thick	1.5 nm-thick chromium coating deposited by evaporation, then exposed to air	greater than a factor of 100 increase in current and greater than 2 V/m decrease in threshold; enhanced emission uniformity	29
MPCVD different ratio of CH_4:H_2 4−6 atomic layers thick		(1) higher ratio of H_2, better FE performance, because of thinner CNSs and sharper edges (2) VGs with Ti substrates are better than VGs with Si substrates because of the high conductivity of the Ti substrate	30
RF ICP-PECVD CH_4:Ar = 1:4	Ar plasma postgrowth treatment for 1, 3, and 5 min, respectively	Ar treatment for 3 min gave best FE performance because it rendered the best shapes	31
RF ICP-PECVD C_2H_2:H_2 = 4:1 2000 nm high 1−2 nm thick		(1) much lower threshold fields, higher current density, compared with the VG made by CH_4 (2) more emitting sites due to uniform sheet height	32
H radical injection PECVD (CCP + SWP) C_2F_6 and H_2 mixture	10 min of postgrowth N_2 plasma treatment	emission current was increased 100 times with the same applied field	33
MPCVD CH_4: N_2 = 1:4	in-situ nitrogen-doping	greater than a factor of 6 increase in max current density at a field of 2.16 V/μm and 0.85 V/μm decrease in turn-on field, in comparison to pristine VG with same configuration	34
MPCVD CH_4: H_2 = 1:5	3 nm-thick Au, Ag, Pd, Ti coating deposited by evaporation in Ar, respectively	Ti has lowest turn on and threshold fields, with a field enhancement factor ∼8300 because of strong interaction between Ti (3d) and graphene (π bands)	35
MPCVD 8−10 layers of graphene at bottom and 2−4 layers at top edge of CNS	30 min of NH_3 plasma postgrowth treatment at 350 °C, resulting a amine (C-NH_2) terminal configuration at edges	1.9 V/μm decrease in turn-on field; more stable emission with fluctuation less than 5%	36

https://dx.doi.org/10.1021/acsami.0c19188
ACS Appl. Mater. Interfaces 2021, 13, 9561−9579

MPCVD uses waveguide transmission, and the electromagnetic field density in the waveguide is relatively low. Due to several technical problems (such as microwave source power being limited, the electromagnetic field density in a 2.45 GHz microwave waveguide is relatively lower than RF coil antenna), the plasma density in RF ICP-PECVD and most MPCVD are similar and their pressure are around 0.1−1 Torr. CCP uses plate electrodes to store energy and discharge. The energy stored in plate electrodes is low, so that the excited plasma density is also low. According to the released working pressure and current, the plasma density of EBEP-PECVD should be between that of ICP-PECVD and CCP-PECVD. TCVD and HWCVD use external heating sources to ionize the carbon source by heating it to extremely high kinetic energy. The concentration of ionized electron and ionized carbon radical is much lower than that in the plasma. Therefore, based on the principles of plasma physics, the plasma density has an order of AHV-PECVD > MPCVD ∼ ICP-PECVD > EBEP-PECVD > CCP-PECVD > magnetron sputtering, and TCVD and HWCVD are plasma-free.

The first obvious trend in the growth process is that a higher plasma density leads to a higher vertical growth rate. PECVD is generally faster than magnetron sputtering, TCVD, and HWCVD. According to the literature, magnetron sputtering only renders a growth rate of less than 1 nm/min. The exceptionally low growth rate of magnetron sputtering results from the low conversion efficiency of ionized carbon radicals to VG. HWCVD renders a growth rate of less than 20 nm/min. AHV-PECVD with a growth rate of several hundred nanometers per minute is faster than most other PECVD synthesis methods, although it is not suitable for VG growth on large and planar substrates due to the nature of atmospherically high voltage discharge. ICP-PECVD and MPCVD have typical growth rates of ∼100 nm/min, which is faster than those of EBEP-PECVD and CCP-PECVD (∼20 nm/min). Second, TE-MPCVD, EBEP-PECVD, and CCP-PECVD are more like to synthesize VG with straight up CNSs. On the other hand, TM-MPCVD, ECR-MPCVD, and ICP-PECVD render a more curved feature of VG. We suppose this observation is strongly related to the motion direction of ionized carbon radicals generated by the plasma, e.g. a motion direction perpendicular to the substrate causes a straight up morphology, and a motion direction parallel to the substrate plane causes a curved morphology. The morphology has a strong correlation with the height limit of VG. Generally speaking, VGs with curved feature have a height limit of about 10 μm, while VGs with straight up features can grow to several tens of microns. Third, with the same synthesis method and other parameters, a lower carbon content, a lower plasma power, or a lower substrate temperature tends to synthesize VG with larger average CNS size and sparser distribution and vice versa. Fourth, a higher content of H_2 as a buffer gas causes thinner CNS of VG. Both edge thickness and average thickness of CNS are factors that affect performance in various applications. Although such observation is only qualitative, due to the limitation of characterization methods, e.g. it is ambiguous to define and measure the average thickness, and lack of systematic quantitative data, this trend is conformed by many prior researches. Based on the above observations, if one wants to rapidly synthesize VG composed of thin, dense, and curved CNSs on a large planar substrate, an optimized approach will be employing CH_4 as carbon source, a large portion of H_2 as buffer gas, high power ICP-PECVD or TM-MPCVD as synthesis methods with high substrate temperature.

A sustainable, low cost, and safe carbon source is another research topic. Other than methods that transform solid carbon compounds (e.g., honey, butter, lard oil, glucose, or urea, etc.) to VG-like-materials by heat or plasma treatment, a successful pioneering work was done by Wang et al., which used remotely located solid-carbon sources.[24,25] The ad-hoc solid carbon sources in this prior research has restricted the method as an industry-capable process. Fu et al. discovered a growth method in which carbon radicals, the building blocks of vertical graphene, are remotely knocked out from the graphite paper by a low-pressure argon-gas radio frequency inductively coupled plasma (RF ICP) without H_2 gas steaming and energetically condense on a variety of substrate materials. This research demonstrates an easier, safer, and more economical approach to mass produce VG, compared to using hydrocarbon and hydrogen gases as precursors.[26]

3. FIELD EMISSION

The field emission (FE) performance of VG has attracted research attention shortly after the discovery of VG, with research results published as early as in 2002, as a new competitor to previous research highlighting carbon nanotubes (CNTs).[6,7] In this application for cold cathodes of vacuum electronic devices (such as sources of high power microwave/RF tubes or particle accelerators), the most obvious characteristic is VG's spiky, dense, sharp, and vertically orientated edges (normal to a growth substrate), while VG's outstanding electrical conductivity and improved contact resistance between substrate and emitter are all favorable to FE performance against those of CNTs.[27] VG was hailed as a 2D edge emitter in favor of 1D CNT point emitters, which were notorious for nonlinear catastrophic damage. Meanwhile, VG also has some intrinsically unfavorable features for FE, e.g. high work function (∼4.8 eV), corrugated shape, and disuniformity. In this section we focus on the methods employed to improve the FE performance of VG, to overcome unfavorable features, as well as some profound features of VG discovered through the studies.

Researchers have employed a variety of methods aiming at a low emission threshold, high emission current density, high field enhancement factor, long lifetime, and high stability of FE. These methods include in situ morphology control by changing the growth conditions, postgrowth morphology modification, doping, and coating with other elements. Table 1 lists some enhanced FE performance of VG emitters via different methods.[28−36] Note that only qualitative comparisons are made in the table because of a lack of universal standards for the measurement of performances, for example, different values were used as the emission threshold currents in different studies. Readers are encouraged to check references for details.

In addition to the enhancement of FE performance in various aspects, these studies revealed some features of VG which have not been reported before or are difficult to measure by traditional characterization methods. In Bagge-Hansen's work, using the slope and vertical intercept, a phenomenological or equivalent emission site area was determined to be 3×10^{-9} cm^2 for a VG emitter with the size of 0.07 cm^2. It is roughly estimated that there are only approximately 700 emission sites per square millimeter (much less than the density of edges) and the max current that each emitter can carry is ∼500 μA.[28] Finite element modeling carried out by

https://dx.doi.org/10.1021/acsami.0c19188
ACS Appl. Mater. Interfaces 2021, 13, 9561−9579

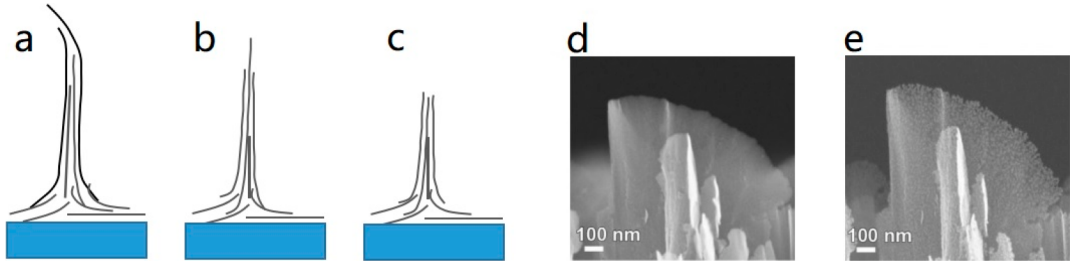

Figure 4. (a–c) Illustration of morphology changes of VG by Ar plasma treatment at different stages.[31] (d, e) SEM images of VG before and after NH_3 plasma treatment [Reprinted with permission from ref 36. Copyright 2016 Elsevier].

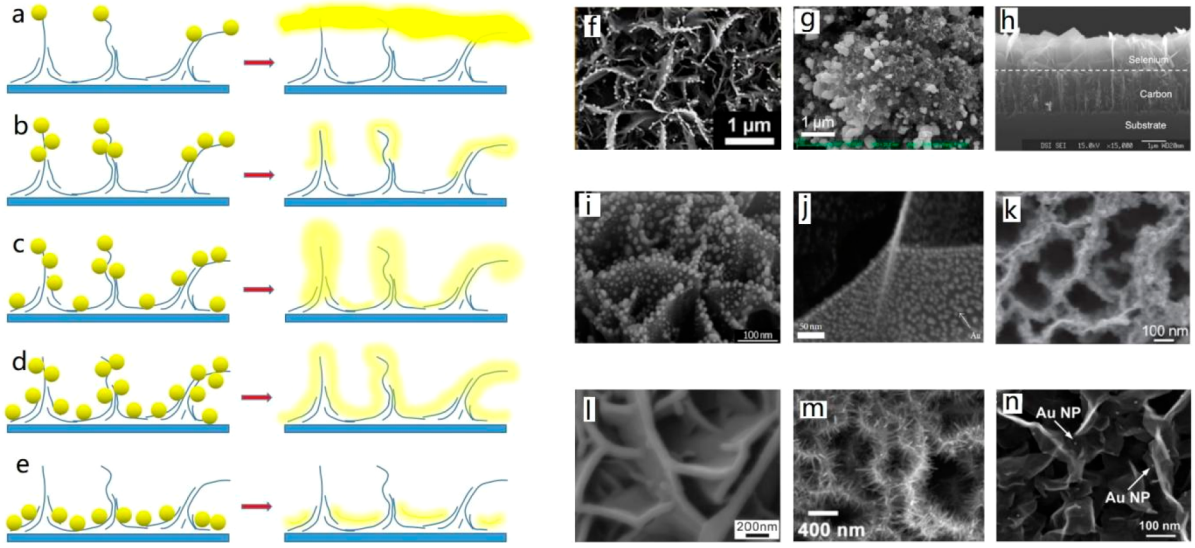

Figure 5. (a–e) five major types of deposition morphologies of functional materials on VG: (left) nanoparticles (NPs), (right) nanolayers. (f) Pt NPs only on edges by electrodeposition. Reprinted with permission from ref 42. Copyright 2012 Wiley-VCH. (g) Ni clusters only on edges by electrodeposition [Reprinted with permission from ref 54. Copyright 2019 Elsevier]. (h) Growth of selenium only on edges [Reprinted with permission from ref 64. Copyright 2004 The Royal Society of Chemistry]. (i) Ag NPs prone to deposit on edges than surfaces by e-beam deposition [Reprinted with permission from ref 52. Copyright 2015 under the terms of the Creative Commons CC BY license]. (j) Au NPs on the surface of CNSs by thermal evaporation deposition [Reprinted with permission from ref 48. Copyright 2015 Hindawi under the terms of Creative Commons Distribution License]. (k) MoS_2 on the surface of CNSs by the solvent thermal method [Reprinted with permission under the terms of the Creative Commons CC BY license from ref 58]. (l) Pt nanolayer on the surface of CNSs by magnetron sputtering [Reprinted with permission from ref 43. Copyright 2010 American Chemical Society]. (m) ZnO seeds conformally grown on VG by atomic layer deposition (ALD), then ZnO nanorods grown on the seeds by hydrothermal reaction [Reprinted with permission from ref 40. Copyright 2019 Elsevier]. (n) Au NPs in concave areas of VG by drop casting [Reprinted with permission from ref 50. Copyright 2013 under the terms of the Creative Commons CC BY license].

Malesevic indicates that, due to electric field screening, only a small percentage of VG edges, which are at least 10% higher than the average height and positioned at a distance of several micrometers from each other, contribute to field emission.[30]

By comparing the FE performance of VG made by CH_4 and C_2H_2, Zhu concluded that, although CNSs of VG have irregular shapes, they follow the trend of Miller's model for knife-edge cathodes. The edge thickness, height, and orientation of the edges all together determine the FE performance.[32] In this study, the VG made by C_2H_2 exhibits sharper and more vertically oriented edges, and a better uniformity in height and morphology, against emitters made by CH_4. Cui systematically studied the FE performance of VG with different synthesis parameters and determined that 300 Pa, 650 °C, and C_2H_2:Ar:H_2 = 3:8:12 are the synthesis parameters most favorable to FE performance.[37] Besides controlling VG's morphology through synthesis parameters, Qi reported that VG's edges can be sharpened and made more uniform using Ar plasma treatment, hence the FE performance was enhanced.[31] Figure 4a–c illustrate the morphology changes of VG by Ar plasma treatment at different stages. Originally, the edges of VG were not vertically orientated which is unfavorable to FE. Ar plasma treatment polished the VG and sharpened the edges, making VG a better emitter. However, too many plasma treatments shortened the CNS, reduced the field intensity, and thus impaired the FE performance. Figure 4d,e are the SEM images of VG before and after NH_3 plasma treatment, showing that defects were created during the treatment.

FE performance enhanced by nitrogen plasma treatment has been reported in multiple studies. Researchers interpreted the mechanism in different ways. Ex-situ XPS analysis carried out by Takeuchi suggested that the incorporated N atoms induce an equivalent increase in the nanodomain size, improvement of the crystallinity, and enhancement of the surface conductivity; thus, the FE performance is enhanced.[33] Zhao indicated that nitrogen doping could significantly increase the π density states near the Fermi level. A ~0.23 eV upward shift of work function was determined by low-energy XPS measurements, which resulted in a lower turn-on field. Meanwhile, nitrogen

https://dx.doi.org/10.1021/acsami.0c19188
ACS Appl. Mater. Interfaces 2021, 13, 9561–9579

functionalization of VG minimized surface desorption and accounted for a more uniform work function distribution.[36] Soin concludes that the enhancement can be attributed to the combined effect of an increase in the surface defects induced by nitrogen plasma, as confirmed by Raman spectroscopy and TEM studies, the shifting of the Fermi level to higher binding energies, and a consequential reduction in the work function, confirmed by VB-XPS as well as Raman spectroscopy.[34]

Besides various in situ and postgrowth treatments, and controlling of growth parameters, growth methods other than ICP-PECVD and MPCVD were also adopted, e.g. radical injection PECVD (CCP and SWP hybrid),[33] hot-filament chemical vapor deposition (HFCVD, similar to HWCVD),[38] and TCVD have also been studied for FE performance.[12,39]

4. FUNCTIONAL MATERIAL LOADING AND APPLICATIONS

In this section, we focus on VG's function to support/carry functional materials such as metal nanoparticles and nanolayers, metal compounds, and enzymes. The functional materials work mainly as catalysts to facilitate the chemical reaction with applications in sensors, hydrogen evolution, and energy conversion. The field enhancement effect of surface plasmon induced by metal nanoparticles will also be mentioned. These implementations mainly utilize VG's large surface area and abundant active sites such as edges and defects. Recall that CNSs (Figure 1a) of VG contribute all the edges, most of the surface area, and most of the defects, as mentioned in the Introduction. In various works, the advantage of using VG as a carrier over other implementations is usually much less loading of functional materials rendering enhancement of orders of magnitude in sensitivity or efficiency. At the same time that we present the recent progresses, we aim at exploring different approaches of depositing functional materials on VG.

It is worth comparing and addressing the pros and cons of each deposition technique used with respect to VG's complex structure. Figure 5 illustrates five common types of deposition morphologies of functional materials on VG, with exemplary SEM images. In the electrodeposition process, usually the nanoparticles first accumulate on the upmost edges of VG because of the electric field distribution induced by VG's morphology. With the increase of loading, the nanoparticles become larger and larger and finally merge into each other forming a sheet over the top of CNSs. The contacts between functional materials and VG are mainly located on the edges of tall CNSs (Figure 5a,f,g,h). There are other types of electric field assisted depositions, e.g. e-beam deposition with bias DC voltage and electrostatic-force directed assembly techniques working in vacuum or atmospheric environments. In these techniques, the nanoparticles also tend to accumulate on the edges because of the electric field distribution. However, having large momentum, some nanoparticles can penetrate deeper into the VG structure and deposit on the surface of CNSs close to the edge (Figure 5b,i). In a magnetron sputtering process, the nanoparticles can penetrate even deeper and render a much more uniform distribution compared to the previous two approaches but still tend to deposit and accumulate on the top and upward surfaces of CNSs especially when the loading gets heavier (Figure 5c,l). The magnetron plasma source needs to be carefully designed if a uniform deposition over a large substrate is desired. Thermal evaporation, hydrothermal deposition, and solvent thermal deposition render similar distributions as magnetron sputtering (Figure 5j,k). Equipment for atomic layer deposition (ALD) are expensive, and the whole coating process is slow. ALD can deliver high conformity coverage on surfaces of VG including the surfaces facing down and deep at the bottom. It can also deliver good uniformity on a large substrate with precise thickness control (Figure 5d). A uniform layer deposited by ALD on VG can further work as a seed layer for the uniform growth of extrusion structures (Figure 5m).[40] Directly dipping VG into chemical solutions renders a relatively uniform distribution, but drop-casting a colloidal solution leads to a deposition at the concave parts of VG (Figure 5e,n). Moreover, chemical reduction of H_2PtCl_6 was employed to deposit PtNPs on VG. A uniform distribution was achieved if VG was treated by Ar plasma before the deposition of platinum nanoparticles (PtNPs). On the other hand, PtNPs only aggregated on the edges if VG was not treated. This work shows that the hydrophilicity is critical to deposition in a wet chemical environment and plasma treatment can enhance the hydrophilicity of VG.[41]

Platinum is the most commonly used catalyst in the hydrogen evolution reaction (HER), with the applications of the hydrogen fuel cell and water electrolysis, and the redox reaction of hydrogen peroxide with the application of a biosensor. It has been proven that using PtNPs can reduce the total amount of platinum load and enhance the efficiency due to the large effective surface area. Based on a VG/PtNPs structure, Claussen reported an electrochemical biosensing application with a limit of detection (LOD) and a sensitivity outperforming PtNPs carried by other kinds of carbon materials, including CNTs and conventional planar graphene.[42] Shang demonstrated an ultralow Pt loading (less than 4.5 $\mu g/cm^2$) electrode outperforming other Pt-carbon based electrodes in the application of methanol fuel cells.[43] Scremin reported a low-cost screen-printed VG/PtNP electrode (Shenzhen Yick Xin Technology Development Ltd. Co.) with 10 times lower loading of Pt yet exhibiting more beneficial HER catalysis than other commercially available Pt-carbon electrodes for water splitting.[44] Zhang reported VG/PtNP electrodes exhibiting significantly enhanced electrocatalytic performance and cycling stability for direct methanol fuel cells and the HER compared to commercial Pt/carbon electrodes.[45] Imai reported a high-durability catalytic electrode composed of VG/PtNPs.[46] In these studies, electrodeposition, magnetron sputtering, ALD, and supercritical fluid metal organic chemical fluid deposition (SCF-MOCFD) were adopted respectively to deposit PtNPs on VG.

The durability of the functional materials deposited on VG is a significant concern as well. In the work of VG/PtNP prepared by SCF-MOCFD, the performance and morphology of PtNP did not change significantly after 20 000 high voltage cyclic voltammogram (CV) cycles, showing great potential for commercialization.[46] VG/PtNPs prepared by ALD also displayed outstanding cycle stability.[45] MoS_2 nanosheets grown on VG through a hydrothermal synthesis were also reported for a super long cycle life as sodium ion battery anodes.[47] We believe that the stability results from the uniform distribution and strong binding between the functional materials and the defects of VG. It also indicates that SCF-MOCFD, ALD, and hydrothermal synthesis tend to build such strong binding.

Gold NPs (AuNPs) have been reported to coat on the VG by thermal evaporation and AuNP colloidal solution drop-

https://dx.doi.org/10.1021/acsami.0c19188
ACS Appl. Mater. Interfaces 2021, 13, 9561−9579

casting. Thermal evaporation renders a uniform distribution of AuNPs on the surface of CNSs of the VG (Figure 5j),[48] while the AuNPs tend to accumulate in the concave areas of the VG's surface by AuNP colloidal solution drop-casting (Figure 5n).[49,50] Surface enhanced Raman spectroscopy (SERS) has been observed on VG/AuNPs because of the localized surface plasmon resonance (LSPR) induced by AuNPs.[51] Furthermore, the VG/AuNP plasmonic hybrid system also exhibits continuum emission from the IR to visible regime which is unusual in plasmonic systems. The authors attributed this to the additional confinement of light by the CNSs of VG. The confinement helps the relaxation of constraints due to the momentum conservation rule by generation of evanescent photons.[49]

Planar graphene carrying noble metal nanoparticles has been proven to facilitate surface enhanced Raman spectroscopy, which is known as the graphene-mediated SERS (G-SERS) effect. Benefiting from VG's large surface area and spatial organizing effect, VG can load more NPs uniformly. The formed three-dimensional (3D) plasmonic structure is expected to result in even stronger G-SERS. With the field enhancement effect of surface plasmon resonance and graphene's further enhancement of plasmonic intensity, a VG/silver nanoparticle (AgNP) structure grown on silicon nanocones attained a plasmon-driven catalytic reaction of *p*-aminothiophenol (PATP) oxidizing to dimercaptoazobenzene (DMAB) which is 4 orders of magnitude more sensitive than previously reported.[52] In this work, AgNPs are deposited on the VG by e-beam deposition. The SEM images show that the AgNPs have a larger concentration on the edge of the VG than on the surfaces (Figure 5i). Cui reported a gas sensor based on the VG/AgNPs composite.[53] In this study, AgNPs were deposited on the VG through an electrostatic-force directed assembly (ESFDA) technique, with a mini-arc plasma reactor. This deposition method is simple and less costly, but the deposited AgNPs are more concentrated on the edge than on the surface of CNSs of VG. Similarly, but with multiple electrodeposition processes for deposition of multiple metals, a glucose sensor based on Cu flakes and Ni particles deposited on VG have achieved a sensitivity of 2 orders of magnitude more than that of other published nonenzymatic glucose sensors in low concentration ranges. Having compared this sensor to a sensor with same Cu and Ni structure but using CNT as carrier, we attribute the higher sensitivity mostly to VG's feature of rich edges because metal particles deposited by electrodeposition tend to concentrate on the edges of VG, which is confirmed by the SEM taken in this study (Figure 5g).[54] Bo reported a VG/SnO_2 sensor for formaldehyde sensing with high sensitivity and low LOD. SnO_2 nanoparticles were electrodeposited from a mixture of 0.2 M $SnCl_4{\cdot}5H_2O$ and 0.16 M HNO_3 by chronoamperometry.[55] Performances of different VG/SnO_2 mass ratios were studied. It was confirmed that, when the loading of SnO_2 reached a certain level, the overall catalytic effect was weakened, indicating a decrease of effective surface area and blocking of gas passage due to the aggregation of SnO_2 particles.

Directional constructions of a VG/nitrogen-doped 1T-2HMoSe_2 composite for efficient hydrogen evolution reaction and a VG/MnO_2 composite for the catalytic decomposition of toluene have been reported.[56,57] The VG/MnO_2 composite rendered significantly higher decomposition of toluene than those of MnO_2 deposited on conventional activated carbon and reduced graphene oxide powders. In the two studies, the functional materials were respectively deposited on VG by hydrothermal techniques and by direct placement of VG into chemical solution with treatments. The functional material nanolayer was uniformly distributed on the surface of VG in both methods, demonstrating themselves as effective approaches for uniform and mass deposition. A similar deposition method called the solvent thermal method also renders uniform deposition of compound on VG (Figure 5k).[58]

VG can also work as carriers for organic macromolecules. A biosensor for lactate detection based on L-lactate oxidase immobilized by chitosan film cross-linked with glutaraldehyde on VG has been reported. It has been demonstrated that the edges and defects of graphene result in high electrocatalytic activity toward several biological applications. In this work, an O_2 plasma treatment further enhanced the amount of enzyme carried on the edges of VG by creating more functional sites and enhancing the hydrophilicity of VG. These effects together resulted in high sensitivity. Together with the flexible nature of VG electrodes, this sensor is proposed to attach to human skin to detect lactate through sweat in real time.[59] A field-effect transistor biosensor was reported with VG coated by AuNP-antibody conjugates. This study gave an example of VG carrying composite functional materials.[50] The fabrication of a H_2O_2 electrochemical sensor with self-cleaning and antibiofouling properties demonstrated that a combined functional material deposition process could lead to multiple features. ALD was employed to deposit a smooth and thin ZnO layer as seeds conformally on the entire VG surface. After that, ZnO nanorods with lengths of ∼300 nm were then grown through hydrothermal reaction, followed by the conformal distribution of ZnO seeds (Figure 5m). Benefiting from its unique hierarchical structure and low surface energy, the VG/nanorod structure displayed superhydrophobicity and showed excellent antifouling properties with high repellence to various fluids.[40]

There are also reports of culturing or attaching various types of live cells on VG.[60−63] Due to the huge size of cells compared to the structure of VG, these cells are only cultured/attached on the edges of VG. Plasma treatments made VG hydrophilic and thus promoted the attachment of the cells. These studies confirm the biocompatibility of VG and propose that VG could work as scaffolding in wider biology applications. To be concluded, the idea of using VG as a scaffold or template for the formation of other types of materials was discovered many years ago[8,64] and is considered as the most promising direction of VG's applications.

5. FLEXIBLE/STRETCHABLE ELECTRODES AND WEARABLE ELECTRONICS APPLICATIONS

Keeping good electrical conductivity when being stretched, compressed, or bent is the basic qualification of flexible/stretchable electrodes. In this section, we focus on wearable electronics composed with VG containing flexible/stretchable electrodes, as well as the mechanisms with which VG's intrinsic features facilitate these applications. Figure 1k,i gives the intuitive concept that VG is conductive, flexible, and stretchable. However, because VG is a thin film material, it has to combine with other elastic materials to form a real device. In practice, VG containing flexible/stretchable electrodes that are made by VG either attaching to a metal foil or embedding into elastomer polymers. The metal foil/VG electrodes mainly display flexibility and the polymer/VG electrodes display both flexibility and stretchability. These VG

https://dx.doi.org/10.1021/acsami.0c19188
ACS Appl. Mater. Interfaces 2021, 13, 9561−9579

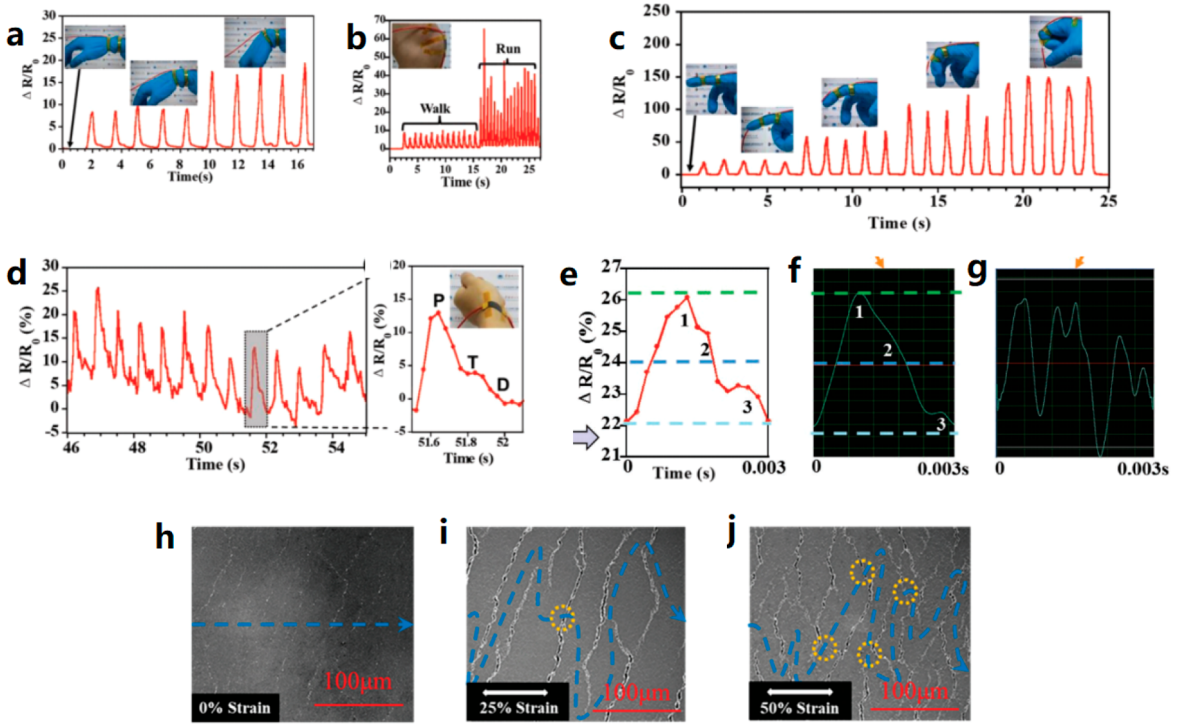

Figure 6. (a–d) Functions realized by VG strain sensors. (e) Single beat curve of a melody measured by a VG strain sensor, (f) original waveform, (g) measured by a commercial microphone [Reprinted with permission from ref 65. Copyright 2019 Wiley-VCH]. (h–j) Microcracks on a basal layer with different strain [Reprinted with permission from ref 68. Copyright 2020 The Royal Society of Chemistry].

containing electrodes play the most important role in the devices that will be mentioned in this section.

Wearable stretch sensors have received widespread attention with the booming wearable smart electronics and robotics market. Advanced wearable strain sensors with both high stretchability and high sensitivity are highly desirable. The sensitivity of strain sensors is characterized by gauge factor, representing the change of a measurable value, e.g. resistance and capacitance, as a function of strain applied. More specifically, the change of resistance as a function of strain is called piezoresistive effect. The stretchability is characterized by maximal strain that can apply to the sensor. A large stretchability indicates a broad sensing range. Benefiting from VG's unique complex structure, wearable sensors made of VG attain both outstanding sensitivity and stretchability simultaneously.[65] Figure 6a–g exhibit some of the sensing functions that have been realized by these sensors.

Wu reported strain sensors consisting of VG sandwiched by two poly(dimethylsiloxane) (PDMS) substrates. Benefiting from the nature of graphene materials, these sensors are insensitive to temperature changes and anticorrosive to human sweat.[66] Furthermore, outperforming most planar graphene based sensors reported previously, the VG sensors simultaneously attain both high sensitivity with a gauge factor of ~32.6 and high stretchability of ~120%, with excellent linearity over the entire detection range. The performance of the sensors was affected by VG's morphology. For example, the sensitivity and stretchability can be tuned by adjusting the height of VG. Sensors consisting of taller VG CNSs display higher sensitivity (gauge factor up to 88.4) but slightly lower stretchability (stretchability up to 55%). Most importantly, Wu revealed that the basal layer of VG played a critical role for the high gauge factor attained by observing the formation of microcracks on the basal layer when strain was applied.

Yang reported a stretchable electronic skin (E-skin) exhibiting a highly sensitive response to joint movement, eye movement, and vocal cord vibration, with a gauge factor of up to 65.9 and a maximum stretchability of 100%, proposing broad potential applications in healthcare, body monitoring, and wearable devices.[67] A polished silicon wafer, an unpolished silicon wafer, and an inverted pyramid-structural silicon wafer were used as substrates to grow VG. The E-skins with VG grown on the unpolished silicon wafer and inverted pyramid-structural silicon wafer exhibited much better stretchability than that on the polished one. Although there was no image released showing the morphology of the down side surface of the basal layer, it is reasonable to assume that a rough and undulating down side surface was formed by the unpolished and inverted pyramid-structural surface of substrates. We make an inference that in addition to the microcracks, the rough and undulating surface of basal layer also accounts for the outstanding gauge factor and stretchability. This mechanism could be compared to a piece of cloth that remains unbroken while being crumpled back and forth and flattened.

Deng further investigated the mechanism that VG that facilitates outstanding sensitivity and stretchability.[65] Microcracks have been formed when VG/PDMS composite is peeled off from the growth substrate. When no strain is applied, the basal layer on both sides of the microcracks contact each other (Figure 6h), thus the current flows directly across the microcracks when a voltage is applied. When the strain sensor is stretched slightly (e.g., 25%), the basal layers on both sides of the microcracks leave each other and the current detours around the microcracks (Figure 6i), in which case, a change of resistance results from the increase of the current path length. When the sensor is further stretched (e.g., 50%), new microcracks are formed and more of the current paths are blocked (Figure 6j); hence, the resistance increases further.

https://dx.doi.org/10.1021/acsami.0c19188
ACS Appl. Mater. Interfaces 2021, 13, 9561–9579

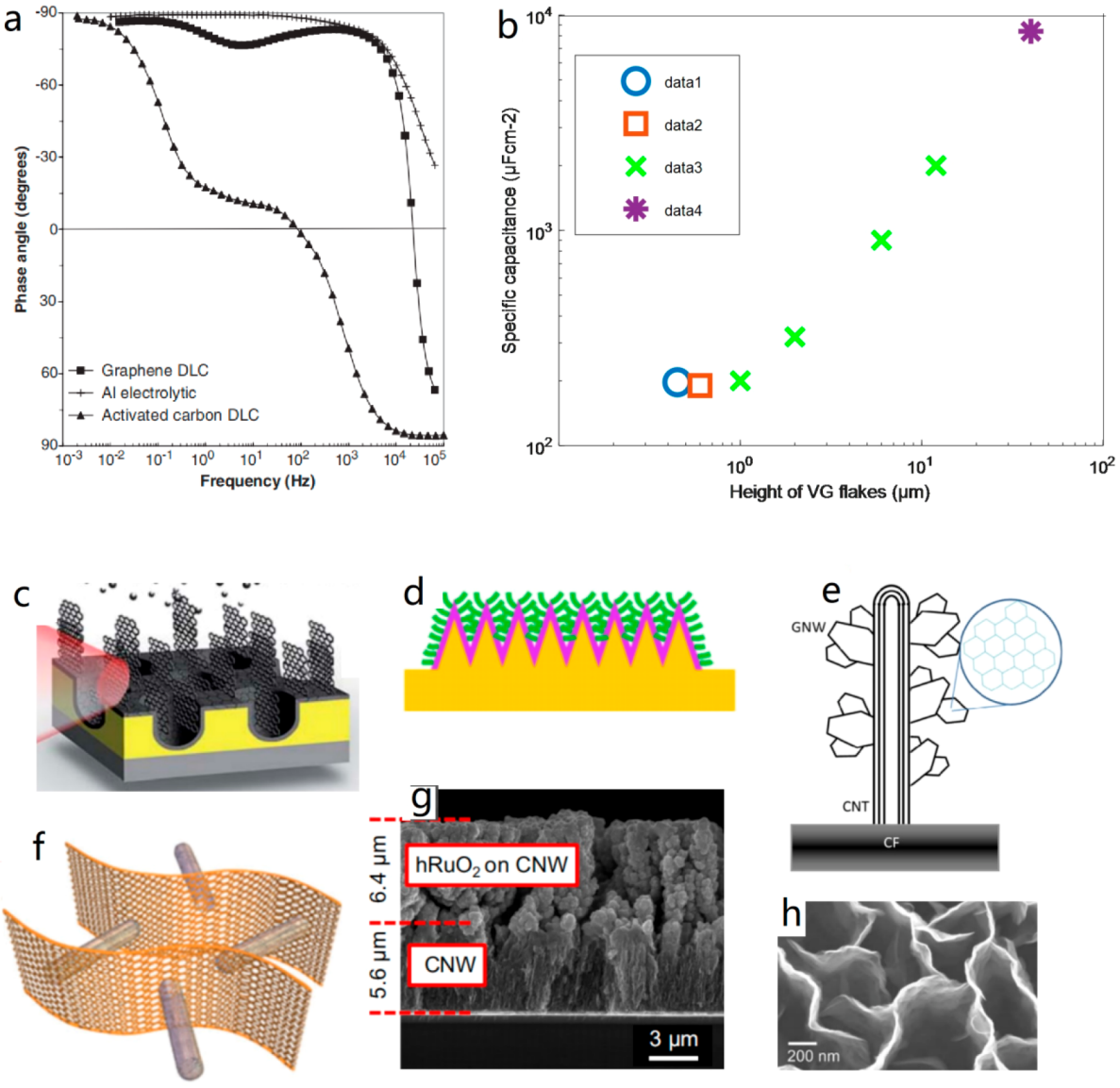

Figure 7. (a) VG EDLC's performance at high frequency approaches to aluminum electrolytic capacitor [Reprinted with permission from ref 78. Copyright 2010 AAAS]. (b) Areal specific capacitance as a function of the height of VG for EDLCs, data 1,[84] data 2,[78] data 3,[80] data 4.[81] (c) Nanocap/VG [Reprinted with permission from ref 86. Copyright 2015 The Royal Society of Chemistry]. (d) Nanocone/VG [Reprinted with permission from ref 87. Copyright 2017 Elsevier]. (e) Carbon nanotube/VG [Reprinted with permission from ref 89. Copyright 2012 Elsevier]. (f) VG/carbon nanotube [Reprinted with permission from ref 88. Copyright 2014 Wiley-VCH]. (g) Mass loading of RuO_2 on VG for ultrahigh areal specific capacitance [Reprinted with permission from ref 102. Copyright 2014 Elsevier]. (h) Sparse loading of RuO_2 on VG for ultrahigh gravimetric specific capacitance [Reprinted with permission from ref 96. Copyright 2017 The Royal Society of Chemistry].

When the sensor is stretched even further (e.g., 100%), there is hardly any detoured current paths remaining on the basal layer and the vertically branched structures (CNSs) of VG are broken at the microcracks. However, the broken vertically branched structures are still in touch with each other, thus the electrode keeps conducting. The above mechanism enables the conductive network to keep functioning to a strain level significantly larger than that of previously reported planar graphene based sensors. In summary, both the basal layer and vertically branched structures of VG contribute to the high sensitivity and stretchability.

The density of microcracks on the basal layer has direct effects on the strain sensors. Two distinct peeling methods were presented to separate a VG/PDMS composite from the growth substrate, which are the ultrasonic peeling (UP) method and the chemical-corroding peeling (CP) method based on the redox reaction between Fe^{3+} and Ni[40]. The UP method leads to high density microcracks on the basal layer while the CP method leads to low density microcracks and keeps the basal layer intact and smooth. These two types of morphologies of the basal layer result in distinct sensing behaviors. Compared to the VG/PDMS sensors prepared by the UP method, the sensors prepared by the CP method exhibit a much lower gauge factor (19.4) with a larger linear strain range (0−100%). Moreover, they exhibit different aging characteristics as 1000 cycles of stretch/release with a maximum strain of 40% were carried out. Sensors prepared by UP method exhibit a more stable gauge factor over cycles, indicating a longer lifetime. This was explained by high density microcracks facilitating the formation of an equilibrium state of

https://dx.doi.org/10.1021/acsami.0c19188
ACS Appl. Mater. Interfaces 2021, 13, 9561−9579

the conductive networks. Piezoresistive strain sensors prepared by the UP method implement multiple functions to detect human physiological signals, such as detecting wrist and finger bending with different angles, distinguishing between walking and running, and identifying a pulse signal. Most interestingly, these sensors were proven to be capable of recognizing the timbre of sounds with frequencies up to 2500 Hz. The waveform obtained by the sensor is much more accurate than that obtained by a commercial microphone (Figure 6e−g). Deng attributed this observation to the high density of microcracks on the basal layer formed by the UP method. These high density microcracks divide the vertical graphene into pieces of much smaller size and thus increase the natural frequency of the sensors greatly to be resonant with the sound to be detected.

In addition to sensors based on piezoresistive effects, a VG capacitive strain sensor prepared by the CP method with a maximum stretchability of ∼80% and a gauge factor of ∼0.97 was reported.[68] Compared to commonly used capacitive strain sensors made of spray-coated Ag nanowires and carbon nanotube (CNT) networks, vertical graphene capacitive strain sensors exhibit better uniformity, which is favorable to quality control and mass production. In addition to recognizing human physiological signals, this capacitive sensor exhibits unique stress direction recognition ability. Morse code transmission was implemented by the sensor.

Another VG strain sensor with stress direction recognition ability was reported by Huang.[69] VG with parallelly aligned CNSs was fabricated by ICP-PECVD. An altering electric field induced by the metal inducers drove the CNSs to align along a specific direction. With the mechanism that has been elaborated above, it is obvious that the in-plane anisotropy of VG's morphology induces an in-plane anisotropy of sensitivity and stretchability, thus enabling sensing of both strain amplitudes and directions. The implementation of this sensor as well as other vertical graphene sensors discussed above reflects the value of VG's unique structure and introduces opportunities to develop advanced wearable sensors.

In a most recent study carried out by Abolpour Moshizi,[70] an ultrasensitive and multifunctional flow sensor was developed based on a VG flexible electrode. Based on the piezoresistive effect elaborated above, the flow sensor is able to distinguish minute changes in the rotational axis, physical geometry, frequency, and amplitude, showing the VG flexible electrode's potential application in medical treatment, movement monitoring, and environmental parameter monitoring.

A temperature sensor based on VG was reported by Yang. The thermal expansion effect of PDMS induces changes of resistance of VG embedded in it, thus the temperature can be measured by monitoring the resistance. Although not showing any advantages over other thermometers, this was the first study reflecting the piezoresistive effect and the stretchability of VG to the best of our knowledge.[71]

Other than the multiple types of sensors mentioned above, VG containing flexible electrodes have been used in flexible supercapacitors,[72−75] flexible potassium ion batteries,[76] flexible lithium−sulfur batteries,[77] and flexible electrochemical biosensors,[59] etc. The flexibility of these devices stems from the mechanisms elaborated above. One interesting thing is that the flexibility is retained after the VG is coated with various functional materials, which heralds broader applications of VG containing flexible/stretchable electrodes.

6. ENERGY STORAGE AND CONVERSION DEVICES

Vertical graphene's applications in electrochemical energy conversion and storage have been summarized elaborately by Zhang.[9] With different perspectives, here we focus on the problems encountered and the approaches of scientists to solve the problems. Some interesting results of the most recent research are included as well.

6.1. Electric Double-Layer Capacitors. The electrode surface area dominantly determines the double-layer capacitance stored per unit voltage in electric double-layer capacitors (EDLCs). The specific surface area of 1000 m^2/g makes VG a good candidate as an EDLC's electrode material along with VG's other intrinsically favorable features. For example, the high electrical conductivity of VG lowers the overall internal resistance and enhances the performance at high frequency, the high chemical stability and corrosion resistance render a long lifetime, and the high thermal conductivity timely transferring the heat to the ambient environment promotes safety. In earlier studies, researchers mainly focused on the high-frequency performance of VG over activated carbon, which is the traditional electrode material for commercial EDLCs. The impedance phase angle of the VG EDLC reached −45° at ∼15 000 Hz in comparison with 0.15 Hz for the activated carbon EDLC, which indicates a much better high-frequency performance of the VG EDLC (Figure 7a).[78] VG's morphology contributes to the performance. Most of the surface area is provided by the CNSs (Figure 1a), and they are exposed and directly accessible, facilitating the transport of the charge. Furthermore, the open structure between the CNSs reduces ionic resistances.

The major problem encountered by VG EDLC is the limited capacitance. It has been reported that pores below 1 nm provide the largest contribution to the capacitance of activated carbon EDLCs,[79] but there is no report that VG's graphitic structure has such a pore distribution. The only report that we have seen is about a calculation carried out by Han based on the density functional theory (DFT) model, which indicates that the pore size distribution of VG used in that certain study has a peak at ∼10 nm, while pores smaller than 2 nm are very limited.[72] This study inspires an interesting question: is the pore size of VG tunable in growth or adjustable by postgrowth treatments. We look forward to seeing progresses in such areas. Another problem is that while facilitating the access to charges, VG's large open structure actually means a low density of CNSs and thus a low effective surface area. Furthermore, the intrinsic hydrophobic nature of VG impedes electrode−electrolyte interaction. Researchers have adopted many methods to enhance capacitance of the VG EDLC. A straightforward approach is to grow VG with larger heights so that more surface area can be achieved for the same substrate surface. For example, Aradilla's work rendered an areal specific capacitance of 2 mF/cm^2 at a current density of 1 mA/cm^2 (∼0.05 Hz) with a VG 12 μm in height.[80] Another example is that an areal specific capacitance of 8.4 mF/cm^2 at a scan rate of 100 mV/s (∼0.05 Hz) was achieved by a 40-μm-high VG.[81] Interestingly, by comparing the values from different research groups, we find that there exists a linear correlation between specific areal capacitance and height of VG (Figure 7b), although the VGs were grown by different parameters and appeared different in morphology. The correlation is specially strong when VGs are more than 1 μm in height, showing a potential for quality control in mass

https://dx.doi.org/10.1021/acsami.0c19188
ACS Appl. Mater. Interfaces 2021, 13, 9561−9579

production. Note that ref 81 demonstrates the tallest VG that we have ever seen. Although it is not clear which kind of microwave was employed in the growth process, the morphology of VG in this study supports our observation in the section of growth process: VGs with straight up features tend to have a larger height limit.

Sahoo et al. demonstrated that surface modification through oxygen plasma exposure could transform the inherent hydrophobic VG surfaces into superhydrophilic ones. In this way, the superhydrophilic VG electrodes revealed a ten-times increase in the areal specific capacitance over the inherent hydrophobic ones. The enhancement in the capacitance is related to the type of the oxygenated functional groups. Hydroxyl and carbonyl type functional groups created by higher plasma powers are demonstrated to be more favorable to capacitance increase, while carboxyl groups possess much lower capacitance.[82] Furthermore, being an oxidizing agent, potassium hydroxide (KOH) grafts the functional groups to the surface and improves the hydrophilicity.[83,84] In these studies, nanopores on VG were observed, and it was believed that these nanopores were formed during the activation process. In the other study, N_2 DC discharge plasma treatment was applied to VG and an enhancement of capacitance up to 6 times was achieved.[85]

Making complex structures on a substrate surface is another common practice to achieve more capacitance. Qi reported a 3D VG-nanocup structured electrode, where nanocups with an average diameter of approximately 800 nm were formed through an annealing process on a Pt film and then VGs were grown on it (Figure 7c). This structure achieved a high specific surface area for ion transmission and storage, and hence, exhibited a high specific capacitance up to three times that of VG on a plane and good cycling stability with about 93% capacitance retention after 3000 cycles.[86] Quan reported 3D VG-Si-nanocone array structured electrodes. Silicon cone arrays with average heights of 900 nm were fabricated by ICP self-masked etching. Then a nickel film was deposited on the silicon cone arrays. Finally, VGs were grown on the nickel film (Figure 7d). The specific capacitance of this structure reaches 0.4 mF/cm^2 at a scan rate of 10 V/s (~5 Hz).[87] Seo presented a hybrid structure formed by the direct growth of carbon nanotubes (CNTs) onto the VG CNS surface (Figure 7e). This hybrid structure showed an overall capacitance of 51.3 mF/cm^2 at a 10 mV/s scan rate.[88] On the contrary, growing VG on CNTs is also an effective approach to enhancing the specific capacitance (Figure 7f).[89,90]

Ma reported a flexible and solid-state VG EDLC using a generic solid gel electrolyte of polyvinyl alcohol (PVA)/H_3PO_4. The capacitance remained unaltered after 100 000 times of bending or 180° folding.[91] Zhang reported an EDLC with features of flexible, solid-state, micro, and in-plane. In this work, ~70 μm thick EDLC was made by graphene with a 3D structure, with (PVA)/H_2SO_4 as a solid gel electrolyte. Both the power density and energy density outperform their counterparts made by graphene oxide (GO) or reduced graphene oxide (rGO). Most importantly, the obtained result showed a capacitance retention of 85% after 5000 cycles at a bend angle of 90°.[92] Note that graphene used in the above two works is not the typical VG being depicted in this article, but they share many common features. These works enlighten the VG EDLC's application in wearable and on-chip electronics. Sahoo made a flexible VG EDLC by sandwiching KOH soaked filter paper with two VG layers. The VG layers were transferred from a nickel substrate, and the basal layers of VG worked perfectly as intrinsic flexible current collectors, which reduced the total thickness and weight of the device.[75]

Commercially available thin-film batteries and micro batteries show a rapid market expansion, but they have a short cycle life and low power and experience safety issues. VG EDLCs are expected to make up for these deficiencies.

6.2. Pseudocapacitors. Pseudocapacitors use metal compounds (metal oxides in most cases) or conducting polymer as electrode materials to accumulate charges by Faradaic reactions. Pseudocapacitors usually have a much higher pseudocapacitance additional to the double-layer capacitance but have a lower charge/discharge rate than EDLCs due to the slow Faradaic reactions. VGs decorated with metal compounds such as MnO_2, RuO_2, TiO_2, CoO_3, $Co(OH)_2$, $Ni(OH)_2$, Fe_2O_3, ZnO_2, TiN, and $TiNb_2O_7$ have been reported as electrode materials of pseudocapacitors.[93−103] In these cases, VG majorly functions as a supporting structure and conduction channel for the metal compounds, considering that most of the compounds have poor long-range electrical conductivity. Besides the features such as large surface area, high electrical conductivity, high chemical stability, and outstanding mechanical strength mentioned in previous sections, VG's unique morphology makes special contributions. The CNSs function as space organizers or regulators preventing aggregation of the electrode materials and providing a large exposed surface area. Furthermore, the openings between CNSs are large enough for access of the electrolyte to the bottom (Figure 1h). Researchers pursue either a high areal specific capacitance or a high gravimetric specific capacitance by introducing VG in their pseudocapacitors.

Taking RuO_2 decorated VG as example, on one hand, Dinh made a pseudocapacitor with energy density comparable to that of lithium-ion microbatteries and areal specific capacitance more than 1000 mF/cm^2 (based on the area of substrate), which is 3 orders of magnitude higher than state-of-the-art micro-supercapacitors, by loading hundreds-of-nanometer-thick RuO_2 on the top 6.4-μm-height-part of CNSs with electrodeposition (Figure 7g). In this case, VG worked as supporter, separator, and current collector, obtaining a high energy storage while maintaining accessibility of the electrolyte.[102] On the other hand, Han loaded RuO_2 with thickness of 3, 5, 10, 20, and 50 nm on VGs by reactive RF magnetron sputtering. This approach attained a gravimetric specific capacitance very close to the theoretical value of RuO_2 which is 2000 F/g when the thickness is 3 and 5 nm, while the gravimetric specific capacitance decreases as the RuO_2 coatings grow thicker (Figure 7h). This study provides a very efficient way to utilize the rare and expensive Ru metal and discloses a trend that the bulkier the electrode material the lower gravimetric specific capacitance.[96] The above two cases generally reflect two types of approaches, which are mass loading with a super large areal specific density by utilizing the height of the VG and sparse loading with a super large gravimetric specific capacitance by utilizing the large surface area of VG. Same as the studies in EDLCs, flexible pseudocapacitors,[74] complicated 3D structures,[93] in-plane and micro capacitors,[103] all solid-state devices,[96,100] and asymmetric supercapacitors based on VG were also reported.[95,104] Two of the most recent studies have provided a new route to further explore VG pseudocapacitors' flexibility, where VG/MnO_2 composites are grown on moldable wires/fibers.[105,106] The idea is to make a 1-dimensional capacitor

https://dx.doi.org/10.1021/acsami.0c19188
ACS Appl. Mater. Interfaces 2021, 13, 9561−9579

with the form of a wire, which can be modified to many shapes to fit the application scenario. Such a design displays better flexibility than traditional 2-dimensional capacitors with planar configurations.

VG has also been applied to enhance the performance of polymer pseudocapacitors.[107,108] A solid-state flexible polymer pseudocapacitor with carbon cloth/VG/PANI as electrodes and polymer gel as electrolyte yields large areal specific capacitance of ~2.6 F/cm^2 and gravimetric specific capacitance of 2000 F/g. This study shows a commercial perspective because its overall performance fills the gap between commercial supercapacitors and lithium thin film batteries.[107] In a most recent study, VG was reported to have a suppressing charge trapping effect in ambipolar conducting polymer (ACP).[109] ACP makes a promising supercapacitor electrode material by transporting both holes and electrons. However, the poor electron transport ability results in charges trapped in the bulky polymers without being sufficiently released, which limits its performance as a supercapacitor electrode material. This is called charge trapping (CT) effect. The CT effect is serious especially when ACP is deposited on a flat surface. During the discharge process of supercapacitors made by ACP, the part adjacent to the current collector first becomes conducting while the charges (especially electrons) relatively far from the current collector are still trapped. The CNSs of VG provide conducting channels to the outer part of ACP, support and distribute the polymer in a three-dimensional way, and thus facilitate transfer of charges and enhanced stability.

6.3. Other Energy Storage/Conversion Devices. Applications of VG for other energy storage devices, e.g. lithium ion batteries and flow batteries have been reported.[9] VG mainly functions as a supporting structure and a binder free conduction bridge to the current collector in these studies. A recent report exhibited a VG supporting structure that could also enhance the stability and cycle life of lithium batteries at high C-rate operation, showing great commercial potential.[110] A study of sodium ion batteries has utilized almost all of VG's beneficial functions mentioned above, i.e. as a space organizer preventing aggregation of MoS_2, as a supporter providing large area, as a conduction channel facilitating the charge transfer, being rich of defects improving sodium ion storage, to enhance the battery's cycle life and high rate performance.[111] An interesting application of VG is in hydrazine fuel cells, which often run into the problem of gas becoming stuck on the surface of the electrode, producing poor electrode efficiency. The morphology of VG provided a rough surface and resolved the problem, leading to a better performance over other carbon based electrodes.[112]

7. OTHER PHYSICAL/CHEMICAL EFFECTS AND NOVEL APPLICATIONS

7.1. Physical Electronics. Graphene displays p-type behavior (electron donation) when interacting with electron-withdrawing groups, such as fluoropolymers, water, nitrogen dioxide, Br_2, and I_2. Accordingly, graphene can form n-type doping when molecules with strong electron-donating ability are adsorbed on the graphene surface.[113] In ambient conditions graphene has been observed to display p-type behavior due to the electron withdrawing nature of adsorbed water. When O_2 is adsorbed on VG, it takes electrons from the graphene, thus the charge carrier concentration of p-type graphene increases. As a result, VG's overall electrical conductivity increases. On the contrary, when H_2 is adsorbed on VG, VG's overall electrical conductivity decreases accordingly. Roy made an ultrasensitive gas sensor based on this mechanism with a metal/insulator/semiconductor (MIS) structure consisting of VG/SiC/p-doped Si. This work achieved an excellent sensitivity of 82 μA/ppm·cm^2, exceptional limit of detection (LOD) of 500 ppb, and ultrafast response of 500 ms. Besides the physical electronic property of graphene materials, the abundant nanographitic edges and defects of VG facilitate the fast electron transfer. The large surface area of VG enables strong adsorption of gas molecules. Furthermore, the porosity of the structure forms passages for gas to penetrate uniformly into the entire VG. All these factors contribute to sensitive, fast, and stable operation.[114] With the same mechanism, an earlier VG gas sensor for NO_2 and NH_3 with planar electrode configuration was reported by Yu.[115] Note that other than the adsorption effect, p-type VG can be made by introducing boron dopants[116] and N-type VG can be made by introducing nitrogen dopants during the growth process.[117]

7.2. Electromagnetism Effects. Zhang reported an interesting phenomenon that when VG was coated on the surface of FeCuNbSiB amorphous ribbons, the field-dependent magnetoimpedance effect was obviously changed. This effect was attributed to the enhancement of transverse permeability induced by the unique morphology of VG. The vertical graphene sheets may depress the eddy current and redistribute the surface magnetic field, which is favorable for improving the transverse permeability.[118]

7.3. Electrochemical Analytical and Catalytic Applications. With chemical stability and good electrical conductivity, carbon electrodes are widely used in electrochemical applications. Electrochemical electrodes composed of graphene and CNTs have drawn research interests because of their rich active sites such as edges and defects and outstanding electrical conductivity. Electrochemical electrodes made by VG are a further upgraded version because of the larger surface area and even more rich active sites compared to planar graphene and CNTs. VG electrochemical electrodes have been used to detect/sense multiple molecules.[119,120]

The sensing system is based on cyclic-voltammetry technology, composed of working, reference, and counter electrodes. A time-dependent potential is applied between the working electrode and the reference electrode, and the resulting current is measured as a function of this potential. Current peaks observed at specific applied voltages are due to specific redox reactions running on the working electrode surface. Redox reactions of different substances have different position on the $I-V$ curve. The concentration and species of certain substances can be sensed by the height and position of the current peaks. In practice, VG is mainly used as the working electrode. VG's large surface area as well as large number of edges and defects enable it to adsorb more of the substance to be sensed. It is specially helpful in the application of electrochemical stripping analysis which is an electrochemical analytic method effective in trace detection of heavy metal pollution and involving an accumulation process of electroactive material at the electrode.[121]

The catalytic effect for oxygen reduction reactions of VG without any doping or functional material carrying has been reported. Being among the highest of pure carbon electrodes, the achieved catalytic effect of VG was attributed to the large amount of defects and edges as well as large accessible surface

https://dx.doi.org/10.1021/acsami.0c19188
ACS Appl. Mater. Interfaces 2021, 13, 9561−9579

area and high electrical conductivity. VG has potential in the application of biofuel cells for the catalytic effect.[122]

7.4. Photon Trapping and Thermal Effects. The dense CNSs endow VG an excellent photon trapping feature. A comprehensive study on light absorption of VG was carried out by Evlashin. When VG is more than 1 μm in height (Figure 1a), it absorbs more than 96% of the light in the wavelength range from 0.4 to 10 μm.[123] The photoluminescence properties of VG have been studied by Wang with a 325 nm-laser-beam as the irradiation source. VG grown on carbon nanotips can further enhance the light absorption, and observed photoluminescence bands at 515−519 nm was attributed to the transition between the π^* and π bands of these carbon nanomaterials, and the strong light trapping effect were proposed to apply in solar cells.[124,125] An ultralow-threshold random laser action from semiconductor nanoparticles assisted by VG is demonstrated. The semiconductor nanoparticles carried by VG work as the gain medium, and the CNSs of VG work as the cavities for trapping the optical photons. The strong photon trapping effect of VG induces ultralow values of threshold energy density. The threshold is further reduced when the photon trapping and strong plasmonic enhancement are combined with coatings of Ag/SiO_2 on the VG.[126] A dynamical photon drag effect (DPDE) resulting from the dynamical transfer of light momentum to the photon generated electron and hole distributions is considered to contribute to the photon trapping feature. Planar and single-layer graphene normally displays a weak DPDE due to its weak light−matter interaction. Zhu reported enhanced and broadband terahertz (THz) emission from VG by DPDE effect due to the complex structure of VG.[127] This study exhibits the potential for high performance THz emitters and THz detectors based on VG.

Based on the photon trapping effect, photothermal heaters at a transmittance range of 97%−34% with a 70%−130% increase in the surface temperature under simulated sunlight irradiation were reported.[128] The transmittance can be controlled by the height of VG growing on soda-lime glasses. Based on the same effect, a flexible thin-film photothermal heater was invented to heat a biochemical reactor.[129] In this application, the outstanding thermal conductivity of VG's basal layers plays a critical role for a very uniform in-plane temperature distribution.

Two studies based on other kinds of graphene materials with similar structures as VG are worth mentioning here. One is about a membrane for highly efficient solar thermal generation of clean water.[130] The other is about a thermal dissipating film with outstanding thermal conductivity in the vertical direction. Although the materials used in these two studies are not typical VG studied in this review, they point out promising application directions for VG.[131]

8. SUMMARY, CHALLENGES, AND PERSPECTIVES

This article has reviewed recent research progress on a novel nanocarbon thin-film material, comprised of vertically free-standing few-layer graphene and carbon nanosheets ("vertical graphene" in this paper for simplicity). This material is distinct from planar growth graphene materials (single-layer or few-layer by CVD processes). Different than 2D crystals, vertical graphene is a complex material with unique 3D hierarchical structures, having abundant out-exposing edges, high porosity, plentiful nanopassages, and ultralarge surface area. Such complex morphology is indispensable for emerging applications in the fields of electrochemistry, bioelectronics, and flexible electronics. Specifically, this article has described how to utilize vertical graphene as field-emission cold cathodes, supercapacitors, electrocatalytic electrodes, wearable strain sensors, optoelectronics, et al.

Vertical graphene had been broadly studied as small samples in academic communities, and the challenges include the following: how to standardize nomenclatures of this complex carbon nanostructure; how to characterize and model its complex hierarchy structure; how to reveal/simulate its growth mechanism-dynamics; and how to integrate the small-sample processing experience to real industry devices in mass production level.

Exploring vertical graphene calls for different approaches than that of CVD growth planar graphene, or graphene nanoplates derived from graphite flakes. Other than legacy PECVD processes to grow vertical graphene, more advanced techniques are emerging from a variety of research groups, such as using solid-state carbon sources (instead of a hydrocarbon gas), or heater-free processes. Some other promising growth methods are under development, by applying magnetic fields in a conventional PECVD chamber for instance.

Commercial applications of vertical graphene might soon proliferate in flexible electronics, bioelectronics, microenergy conversion and storage, electrocatalyst loading, biochemical sensors, electrochemical analysis, and wearable devices. We believe that vertical graphene thin-film carbon nanomaterials will be more promising in terms of research and commercialization, compared to conventional graphene and/carbon nanotube materials.

AUTHOR INFORMATION

Corresponding Author

Wenjie Fu − *School of Electronic Science and Engineering, University of Electronic Science and Technology of China, Chengdu, Sichuan 610054, China; William and Mary Research Institute, College of William and Mary, Williamsburg, Virginia 23187, United States;* orcid.org/0000-0003-4321-4757; Email: fuwenjie@uestc.edu.cn

Authors

Wei Zheng − *School of Electronic Science and Engineering, University of Electronic Science and Technology of China, Chengdu, Sichuan 610054, China; William and Mary Research Institute, College of William and Mary, Williamsburg, Virginia 23187, United States*

Xin Zhao − *William and Mary Research Institute, College of William and Mary, Williamsburg, Virginia 23187, United States*

Complete contact information is available at: https://pubs.acs.org/10.1021/acsami.0c19188

Notes

The authors declare no competing financial interest.

ACKNOWLEDGMENTS

This work was supported by the National Key Research and Development Program of China under 2019YFA0210202, the National Natural Science Foundation of China under Grant 61971097.

https://dx.doi.org/10.1021/acsami.0c19188
ACS Appl. Mater. Interfaces 2021, 13, 9561−9579

REFERENCES

(1) Ando, Y.; Zhao, X.; Ohkohchi, M. Production of petal-like graphite sheets by hydrogen arc discharge. *Carbon* **1997**, *35*, 153.

(2) Hiramatsu, M.; Hori, M. *Carbon Nanowalls Synthesis and Emerging Applications*; Springer, 2010.

(3) Chen, J.; Bo, Z.; Lu, G. H. *Vertically-Oriented Graphene PECVD Synthesis and Applications*; Springer, Switzerland, 2015.

(4) Zhu, M. Y. *Carbon Nanosheets and Carbon Nanotubes by RF PECVD*. Ph.D. Thesis, The College of William and Mary, Virginia, USA, 2006.

(5) Wu, Y. H.; Qiao, P. W.; Chong, T. C.; Shen, Z. X. Carbon Nanowalls Grown by Microwave Plasma Enhanced Chemical Vapor Deposition. *Adv. Mater.* **2002**, *14*, 64.

(6) Shang, N. G.; Au, F. C. K.; Meng, X. M.; Lee, C. S.; Bello, I.; Lee, S. T. Uniform Carbon Nanoflake Films and Their Field Emissions. *Chem. Phys. Lett.* **2002**, *358*, 187.

(7) Wang, J. J.; Zhu, M. Y.; Outlaw, R. A.; Zhao, X.; Manos, M. D.; Holloway, B. C.; Mammana, V. P. Free-standing Subnanometer Graphite Sheets. *Appl. Phys. Lett.* **2004**, *85*, 1265.

(8) Wu, Y. H.; Yang, B. J.; Han, G. C.; Zong, B. Y.; Ni, H. Q.; Luo, P.; Chong, T. C.; Low, T. S.; Shen, Z. X. Fabrication of a Class of Nanostructured Materials Using Carbon Nanowalls as the Templates. *Adv. Funct. Mater.* **2002**, *12*, 489.

(9) Zhang, Z. Y.; Lee, C. S.; Zhang, W. J. Vertically Aligned Graphene Nanosheet Arrays: Synthesis, Properties and Applications in Electrochemical Energy Conversion and Storage. *Adv. Mater.* **2017**, *7*, 1700678.

(10) Seo, D. H.; Rider, A. E.; Kumar, S.; Randeniya, L. K.; Ostrikov, K. Vertical Graphene Gas- and Bio-sensors Via Catalyst-free, Reactive Plasma Reforming of Natural Honey. *Carbon* **2013**, *60*, 221.

(11) Bo, Z.; Cui, S. M.; Yu, K. H.; Lu, G. H.; Mao, S.; Chen, J. H. Note: Continuous Synthesis of Uniform Vertical Graphene on Cylindrical Surfaces. *Rev. Sci. Instrum.* **2011**, *82*, No. 086116.

(12) Guo, X.; Qin, S. C.; Bai, S.; Yue, H. W.; Li, Y. L.; Chen, Q.; Li, J. S.; He, D. Y. Vertical Graphene Nanosheets Synthesized by Thermal Chemical Vapor Deposition and the Field Emission Properties. *J. Phys. D: Appl. Phys.* **2016**, *49*, 385301.

(13) Zheng, S. H.; Li, Z. L.; Wu, Z. S.; Dong, Y. F.; Zhou, F.; Wang, S.; Fu, Q.; Sun, C. L.; Guo, L. W.; Bao, S. H. High Packing Density Unidirectional Arrays of Vertically Aligned Graphene with Enhanced Areal Capacitance for High-Power Micro-Supercapacitors. *ACS Nano* **2017**, *11*, 4009.

(14) Deng, J. H.; Wu, S. L.; Yang, Y. M.; Zheng, R. T.; Cheng, G. A. Fabricating Vertically Aligned Ultrathin Graphene Nanosheets Without Any Catalyst Using RF Sputtering Deposition. *Nucl. Instrum. Methods Phys. Res., Sect. B* **2013**, *307*, 177.

(15) Shimabukuro, S.; Hatakeyama, Y.; Takeuchi, M.; Itoh, T.; Nonomura, S. Preparation of Carbon Nanowall by Hot-Wire Chemical Vapor Deposition and Effects of Substrate Heating Temperature and Filament Temperature. *Jpn. J. Appl. Phys.* **2008**, *47*, 8635.

(16) Shiji, K.; Hiramatsu, M.; Enomoto, A.; Nakamura, M.; Amano, H.; Hori, M. Vertical Growth of Carbon Nanowalls Using RF Plasma-enhanced Chemical Vapor Deposition. *Diamond Relat. Mater.* **2005**, *14*, 831.

(17) Kondo, S.; Hori, M.; et al. Highly Reliable Growth Process of Carbon Nanowalls Using Radical Injection Plasma-enhanced Chemical Vapor Deposition. *J. Vac. Sci. Technol. B* **2008**, *26*, 1294.

(18) Mori, T.; Hiramatsu, M.; Yamakawa, K.; Takeda, K.; Hori, M. Fabrication of Carbon Nanowalls Using Electron Beam Excited Plasma-enhanced Chemical Vapor Deposition. *Diamond Relat. Mater.* **2008**, *17*, 1513−1517.

(19) Wu, Y. H.; Yu, T.; Shen, Z. X. Two-dimensional Carbon Nanostructures: Fundamental Properties, Synthesis, Characterization, and Potential Applications. *J. Appl. Phys.* **2010**, *108*, No. 071301.

(20) Chuang, A. T. H.; Boskovic, B. O.; Robertson, J. Freestanding Carbon Nanowalls by Microwave Plasma-enhanced Chemical Vapour Deposition. *Diamond Relat. Mater.* **2006**, *15*, 1103−1106.

(21) Thomas, R.; Rao, G. M. Synthesis of 3-dimensional Porous Graphene Nanosheets Using Electron Cyclotron Resonance Plasma Enhanced Chemical Vapour Deposition. *RSC Adv.* **2015**, *5*, 84927−84935.

(22) Wang, J. J.; Zhu, M. Y.; Outlaw, R. A.; Zhao, X.; Manos, D. M.; Holloway, B. C. Synthesis of Carbon Nanosheets by Inductively Coupled Radio-frequency Plasma Enhanced Chemical Vapor Deposition. *Carbon* **2004**, *42*, 2867−2872.

(23) Sato, G.; Morio, T.; Kato, T.; Hatakeyama, R. Fast Growth of Carbon Nanowalls from Pure Methane using Helicon Plasma-Enhanced Chemical Vapor Deposition. *Jpn. J. Appl. Phys.* **2006**, *45*, 5210−5212.

(24) Wang, Z. P.; Shoji, M.; Baba, K.; Ito, T.; Ogata, H. Microwave Plasma-assisted Regeneration of Carbon Nanosheets with Bi- and Trilayer of Graphene and Their Application to Photovoltaic Cells. *Carbon* **2014**, *67*, 326−335.

(25) Wang, Z.; Ogata, H.; Morimoto, S.; Fujishige, M.; Takeuchi, K.; Hashimoto, Y.; Endo, M. Synthesis of Carbon Nanosheets from Kapton Polyimide by Microwave Plasma Treatment. *Carbon* **2014**, *72*, 421−424.

(26) Fu, W. J.; Zhao, X.; Zheng, W. Growth of Vertical Graphene Materials by an Inductively Coupled Plasma with Solid-state Carbon Sources. *Carbon* **2021**, *173*, 91−96.

(27) Jiang, L. L.; Yang, T. Z.; Liu, F.; Dong, J.; Yao, Z. H.; Shen, C. M.; Deng, S. Z.; Xu, N. S.; Liu, Y. Q.; Gao, H. J. Controlled Synthesis of Large-Scale, Uniform, Vertically Standing Graphene for High-Performance Field Emitters. *Adv. Mater.* **2013**, *25*, 250−255.

(28) Bagge-Hansen, M.; Outlaw, R. A.; Miraldo, P.; Zhu, M. Y.; Hou, K.; Theodore, N. D.; Zhao, X.; Manos, D. M. Field emission from Mo_2C coated carbon nanosheets. *J. Appl. Phys.* **2008**, *103*, No. 014311.

(29) Hou, K.; Outlaw, R. A.; Wang, S.; Zhu, M. Y.; Quinlan, R. A.; Manos, D. M.; Kordesch, M. E.; Arp, U.; Holloway, B. C. Uniform and Enhanced Field Emission from Chromium Oxide Coated Carbon Nanosheets. *Appl. Phys. Lett.* **2008**, *92*, 133112.

(30) Malesevic, A.; Kemps, R.; Vanhulsel, A.; Chowdhury, M. P.; Volodin, A.; Haesendonck, C. V. Field Emission From Vertically Aligned Few-layer Graphene. *J. Appl. Phys.* **2008**, *104*, No. 084301.

(31) Qi, J. L.; Wang, X.; Zheng, W. T.; Tian, H. W.; Hu, C. Q.; Peng, Y. S. Ar Plasma Treatment On Few Layer Graphene Sheets For Enhancing Their Field Emission Properties. *J. Phys. D: Appl. Phys.* **2010**, *43*, No. 055302.

(32) Zhu, M.Y.; Outlaw, R.A.; Bagge-Hansen, M.; Chen, H.J.; Manos, D.M. Enhanced Field Emission of Vertically Oriented Carbon Nanosheets Synthesized by C_2H_2/H_2 Plasma Enhanced CVD. *Carbon* **2011**, *49*, 2526−2531.

(33) Takeuchi, W.; Kondo, H.; Obayashi, T.; Hiramatsu, M.; Hori, M. Electron Field Emission Enhancement of Carbon Nanowalls by Plasma Surface Nitridation. *Appl. Phys. Lett.* **2011**, *98*, 123107.

(34) Soin, N.; Roy, S. S.; Roy, S.; Hazra, K. S.; Misra, D. S.; Lim, T. H.; Hetherington, C. J.; McLaughlin, J. A. Enhanced and Stable Field Emission from in Situ Nitrogen-Doped Few-Layered Graphene Nanoflakes. *J. Phys. Chem. C* **2011**, *115*, 5366−5372.

(35) Kaushik, V.; Shukla, A. K.; Vankar, V. D. Improved Electron Field Emission From Metal Grafted Graphene Composites. *Carbon* **2013**, *62*, 337−345.

(36) Zhao, C. X.; Zhang, Y.; Deng, S. Z.; Xu, N. S.; Chen, J. Surface Nitrogen Functionality For the Enhanced Field Emission of Free-standing Few-layer Graphene Nanowalls. *J. Alloys Compd.* **2016**, *672*, 433−439.

(37) Cui, L. F.; Chen, J. T.; Yang, B. J.; Sun, D. F.; Jiao, T. F. RF-PECVD Synthesis of Carbon Nanowalls and Their Field Emission Properties. *Appl. Surf. Sci.* **2015**, *357*, 1−7.

(38) Behura, S. K.; Mukhopadhyay, I.; Hirose, A.; Yang, Q. Q.; Jani, O. Vertically Oriented Few-layer Graphene as an Electron Field-Emitter. *Phys. Status Solidi A* **2013**, *210*, 1817−1821.

(39) Wang, H. P.; Gao, E. L.; Liu, P.; Zhou, D. L.; Geng, D. C.; Xue, X. D.; Wang, L. P.; Jiang, K. L.; Xu, Z. P.; Yu, G. Facile Growth of

https://dx.doi.org/10.1021/acsami.0c19188
ACS Appl. Mater. Interfaces 2021, 13, 9561−9579

Vertically-aligned Graphene Nanosheets Via Thermal CVD: The Experimental And Theoretical Investigations. *Carbon* **2017**, *121*, 1−9.
(40) Hang, T.; Xiao, S.; Yang, C.; Li, X. L.; Guo, C.; He, G.; Li, B. H.; Yang, C. D.; Chen, H. J.; Liu, F. M.; Deng, S. Z.; Zhang, Y.; Xie, X. Hierarchical Graphene/nanorods-based H_2O_2 Electrochemical Sensor With Self-cleaning and Anti-biofouling properties. *Sens. Actuators, B* **2019**, *289*, 15.
(41) Tomatsu, M.; Hiramatsu, M.; Foord, J. S.; Kondo, H.; Ishikawa, K.; Sekine, M.; Takeda, K.; Hori, M. Hydrogen Peroxide Sensor Based On Carbon Nanowalls Grown by Plasma-enhanced Chemical Vapor Deposition. *Jpn. J. Appl. Phys.* **2017**, *56*, No. 06HF03.
(42) Claussen, J. C.; Kumar, A.; Jaroch, D. B.; Khawaja, M. H.; Hibbard, A. B.; Porterfield, D. M.; Fisher, T. S. Nanostructuring Platinum Nanoparticles on Multilayered Graphene Petal Nanosheets for Electrochemical Biosensing. *Adv. Funct. Mater.* **2012**, *22*, 3399−3405.
(43) Shang, N. G.; Papakonstantinou, P.; Wang, P.; Silva, S. R. P. Platinum Integrated Graphene for Methanol Fuel Cells. *J. Phys. Chem. C* **2010**, *114*, 15837−15841.
(44) Scremin, J.; Joviano dos Santos, I. V.; Hughes, J. P.; García-Miranda Ferrari, A.; Valderrama, E.; Zheng, W.; Zhong, X. Z.; Zhao, X.; Crapnell, R. D.; Rowley-Neale, S. J.; Banks, C. E.; et al. Platinum nanoparticle decorated vertically aligned graphene screen-printed electrodes: electrochemical characterisation and exploration towards the hydrogen evolution reaction. *Nanoscale* **2020**, *12*, 18214−18224.
(45) Zhang, H. F.; Ren, W. N.; Guan, C.; Cheng, C. W. Pt Decorated 3D Vertical Graphene Nanosheet Arrays for Efficient Methanol Oxidation and Hydrogen Evolution Reactions. *J. Mater. Chem. A* **2017**, *5*, 22004−22011.
(46) Imai, S.; Kondo, H.; Cho, H.; Kano, H.; Ishikawa, K.; Sekine, M.; Hiramatsu, M.; Ito, M.; Hori, M. High-durability Catalytic Electrode Composed of Pt Nanoparticle-supported Carbon Nanowalls Synthesized by Radical-injection Plasma-enhanced Chemical Vapor Deposition. *J. Phys. D: Appl. Phys.* **2017**, *50*, 40LT01.
(47) Ren, W. N.; Zhang, H. F.; Guan, C.; Cheng, C. W. Ultrathin MoS2 Nanosheets@Metal Organic Framework-Derived N-Doped Carbon Nanowall Arrays as Sodium Ion Battery Anode with Superior Cycling Life and Rate Capability. *Adv. Funct. Mater.* **2017**, *27*, 1702116.
(48) Mcleod, A.; Kumar, S.; Vernon, K. C.; Ostrikov, K. Vertical Graphene Nanosheets Coated with Gold Nanoparticle Arrays: Effect of Interparticle Spacing on Optical Response. *J. Nanomater.* **2015**, *2015*, 230987.
(49) Sivadasan, A. K.; Parida, S.; Ghosh, S.; Pandian, R.; Dhara, S. Spectroscopically Forbidden Infra-red Emission in Au-vertical Graphene Hybrid Nanostructures. *Nanotechnology* **2017**, *28*, 465703.
(50) Mao, S.; Yu, K. H.; Chang, J. B.; Steeber, D. A.; Ocola, L. E.; Chen, J. H. Direct Growth of Vertically-oriented Graphene for Field-Effect Transistor Biosensor. *Sci. Rep.* **2013**, *3*, 1696.
(51) Mcleod, A.; Vernon, K. C.; Rider, A. E.; Ostrikov, K. Optical Coupling of Gold Nanoparticles on Vertical Graphenes to Maximize SERS Response. *Opt. Lett.* **2014**, *39*, 2334−2337.
(52) Zhao, J.; Sun, M. T.; Liu, Z.; Quan, B. G.; Gu, C. Z.; Li, J. J. Three Dimensional Hybrids of Vertical Graphene-nanosheet Sandwiched by Ag-nanoparticles for Enhanced Surface Selectively Catalytic Reactions. *Sci. Rep.* **2015**, *5*, 16019.
(53) Cui, S. M.; Guo, X. R.; Ren, R.; Zhou, G. H.; Chen, J. H. *J.* Decoration of Vertical Graphene with Aerosol Nanoparticles for Gas Sensing. *J. Phys. D: Appl. Phys.* **2015**, *48*, 314008.
(54) Cui, D. D.; Su, L.; Li, H. J.; Li, M. J.; Li, C. P.; Xu, S.; Qian, L. R.; Yang, B. H. Non-enzymatic Glucose Sensor Based on Micro-/nanostructured Cu/Ni Deposited on Graphene Sheets. *J. Electroanal. Chem.* **2019**, *838*, 154−162.
(55) Bo, Z.; Yuan, M.; Mao, S.; Chen, X.; Yan, J. H.; Cen, K. F. Decoration of Vertical Graphene with Tin Dioxide Nanoparticles for Highly Sensitive Room Temperature Formaldehyde Sensing. *Sens. Actuators, B* **2018**, *256*, 1011−1020.
(56) Deng, S. J.; Zhong, Y.; Zeng, Y. X.; Wang, Y. D.; Yao, Z. J.; Yang, F.; Lin, S. W.; Wang, X. L.; Lu, X. H.; Xia, X. H.; Tu, J. P. Directional Construction of Vertical Nitrogen-Doped 1T-2H MoSe2/Graphene Shell/Core Nanoflake Arrays for Efficient Hydrogen Evolution Reaction. *Adv. Mater.* **2017**, *29*, 1700748.
(57) Yang, S. L.; Bo, Z.; Yang, H. C.; Shuai, X. R.; Qi, H. L.; Li, X. D.; Yan, J. H.; Cen, K. F. Hierarchical Petal-on-Petal MnO2/Vertical Graphene Foam for Postplasma Catalytic Decomposition of Toluene with High Efficiency and Ultralow Pressure Drop. *Ind. Eng. Chem. Res.* **2018**, *57*, 15291−15300.
(58) Wang, Y.; Chen, B.; Seo, D. H.; Han, Z. J.; Wong, J. I.; Ostrikov, K.; Zhang, H.; Yang, H. Y. MoS2-coated Vertical Graphene Nanosheet for High-performance Rechargeable Lithium-ion Batteries and Hydrogen Production. *NPG Asia Mater.* **2016**, *8*, e268.
(59) Chen, Q. W.; Sun, T.; Song, X. F.; Ran, Q. C.; Yu, C. S.; Yang, J.; Feng, H.; Yu, L. Y.; Wei, D. P. Flexible Electrochemical Biosensors Based on Graphene Nanowalls for the Real-time Measurement of Lactate. *Nanotechnology* **2017**, *28*, 315501.
(60) Watanabe, H.; Kondo, H.; Okamoto, Y.; Hiramatsu, M.; Sekine, M.; Baba, Y.; Hori, M. Carbon Nanowall Scaffold to Control Culturing of Cervical Cancer Cells. *Appl. Phys. Lett.* **2014**, *105*, 244105.
(61) Stancu, E. C.; Stanciuc, A. M.; Vizireanu, S.; Luculescu, C.; Moldovan, L.; Achour, A.; Dinescu, G. Plasma Functionalization of Carbon Nanowalls and its Effect on Attachment of Fibroblast-like Cells. *J. Phys. D: Appl. Phys.* **2014**, *47*, 265203.
(62) Ion, R.; Vizireanu, S.; Stancu, C. E.; Luculescu, C.; Cimpean, A.; Dinescu, G. Surface Plasma Functionalization Influences Macrophage Behavior on Carbon Nanowalls. *Mater. Sci. Eng., C* **2015**, *48*, 118−125.
(63) Ion, R.; Vizireanu, S.; Luculescu, C.; Cimpean, A.; Dinescu, G. Vertically, Interconnected Carbon Nanowalls as Biocompatible Scaffolds for Osteoblast Cells. *J. Phys. D: Appl. Phys.* **2016**, *49*, 274004.
(64) Wu, Y. H.; Yang, B. J.; Zong, B. Y.; Sun, H.; Shen, Z. X.; Feng, Y. P. Carbon Nanowalls and Related Materials. *J. Mater. Chem.* **2004**, *14*, 469−477.
(65) Deng, C. H.; Gao, P. X.; Lan, L. F.; He, P. H.; Zhao, X.; Zheng, W.; Chen, W. S.; Zhong, X. Z.; Wu, Y. H.; Liu, L.; Peng, J. B.; Cao, Y. Ultrasensitive and Highly Stretchable Multifunctional Strain Sensors with Timbre-Recognition Ability Based on Vertical Graphene. *Adv. Funct. Mater.* **2019**, *29*, 1907151.
(66) Wu, S. Y.; Peng, S. H.; Han, Z. J.; Zhu, H. W.; Wang, C. H. Ultrasensitive and Stretchable Strain Sensors Based on Mazelike Vertical Graphene Network. *ACS Appl. Mater. Interfaces* **2018**, *10*, 36312−36322.
(67) Yang, J.; Ran, Q. C.; Wei, D. P.; Sun, T.; Yu, L. Y.; Song, X. F.; Pu, L. C.; Shi, H. F.; Du, C. L. Three-dimensional Conformal Graphene Microstructure for Flexible and Highly Sensitive Electronic Skin. *Nanotechnology* **2017**, *28*, 115501.
(68) Deng, C. H.; Lan, L. F.; He, P. H.; Ding, C. C.; Chen, B. Z.; Zheng, W.; Zhao, X.; Chen, W. S.; Zhong, X. Z.; Li, M.; Tao, H.; Peng, J. B.; Cao, Y. High-performance Capacitive Strain Sensors With Highly Stretchable Vertical Graphene Electrodes. *J. Mater. Chem. C* **2020**, *8*, 5541−5546.
(69) Huang, S.; He, G.; Yang, C.; Wu, J. M.; Guo, C.; Hang, T.; Li, B. H.; Yang, C. D.; Liu, D.; Chen, H. J.; Wu, Q. N.; Gui, X. C.; Deng, S. Z.; Zhang, Y.; Liu, F. M.; et al. Stretchable Strain Vector Sensor Based on Parallelly Aligned Vertical Graphene. *ACS Appl. Mater. Interfaces* **2019**, *11*, 1294−1302.
(70) Abolpour Moshizi, S.; Azadi, S.; Belford, A.; Razmjou, A.; Wu, S.; Han, Z. J.; Asadnia, M. Development of an Ultra-Sensitive and Flexible Piezoresistive Flow Sensor Using Vertical Graphene Nanosheets. *Nano-Micro Lett.* **2020**, *12*, 109.
(71) Yang, J.; Wei, D. P.; Tang, L. L.; Song, X. F.; Luo, W.; Chu, J.; Gao, T. P.; Shi, H. F.; Du, C. L. Wearable temperature sensor based on graphene nanowalls. *RSC Adv.* **2015**, *5*, 25609−25615.
(72) Han, Z. J.; Pineda, S.; Murdock, A. T.; Seo, D. H.; Ostrikov, K.; Bendavid, A. RuO_2-coated Vertical Graphene Hybrid Electrodes for High-performance Solid-state Supercapacitors. *J. Mater. Chem. A* **2017**, *5*, 17293−17301.

https://dx.doi.org/10.1021/acsami.0c19188
ACS Appl. Mater. Interfaces 2021, 13, 9561−9579

(73) Chi, K.; Zhang, X. Y.; Tian, X.; Zhang, Z. Y.; Wu, Z.; Xiao, F.; Wang, S. High-Performance Flexible Asymmetric Supercapacitors Facilitated by N-doped Porous Vertical Graphene Nanomesh Arrays. *ChemElectroChem* **2020**, *7*, 362.
(74) He, Y. M.; Chen, W. J.; Li, X. D.; Zhang, Z. X.; Fu, J. C.; Zhao, C. H.; Xie, E. Q. Freestanding Three-Dimensional Graphene/MnO2 Composite Networks As Ultralight and Flexible Supercapacitor Electrodes. *ACS Nano* **2013**, *7*, 174−182.
(75) Sahoo, G.; Ghosh, S.; Polaki, S. R.; Mathews, T.; Kamruddin, M. Scalable Transfer of Vertical Graphene Nanosheets for Flexible Supercapacitor Applications. *Nanotechnology* **2017**, *28*, 415702.
(76) Jin, J.; Cai, W. L.; Cai, J. S.; Shao, Y. L.; Song, Y. Z.; Xia, Z.; Zhang, Q.; Sun, J. Y. MOF-derived Hierarchical CoP Nanoflakes Anchored on Vertically Erected Graphene Scaffolds as Self-supported and Flexible Hosts for Lithium−sulfur Batteries. *J. Mater. Chem. A* **2020**, *8*, 3027−3034.
(77) Qiu, W. D.; Xiao, H. B.; Li, Y.; Lu, X. H.; Tong, Y. X. Nitrogen and Phosphorus Codoped Vertical Graphene/Carbon Cloth as a Binder-Free Anode for Flexible Advanced Potassium Ion Full Batteries. *Small* **2019**, *15*, 1901285.
(78) Miller, J. R.; Outlaw, R. A.; Holloway, B. C. Graphene Double-Layer Capacitor with ac Line-Filtering Performance. *Science* **2010**, *329*, 1637−1639.
(79) Heimböckel, R.; Hoffmann, F.; Fröba, M. Insights into the Influence of the Pore Size and Surface Area of Activated Carbons on the Energy Storage of Electric Double Layer Capacitors with a New Potentially Universally Applicable Capacitor Model. *Phys. Chem. Chem. Phys.* **2019**, *21*, 3122−3133.
(80) Aradilla, D.; Delaunay, M.; Sadki, S.; Gérard, J. M.; Bidan, G. Vertically Aligned Graphene Nanosheets on Silicon Using an Ionic Liquid Electrolyte: Towards High Performance On-chip Micro-supercapacitors. *J. Mater. Chem. A* **2015**, *3*, 19254−19262.
(81) Zhang, Y.; Zou, Q. H.; Hsu, H. S.; Raina, S.; Xu, Y. X.; Kang, J. B.; Chen, J.; Deng, S. Z.; Xu, N. S.; et al. Morphology Effect of Vertical Graphene on the High Performance of Supercapacitor Electrode. *ACS Appl. Mater. Interfaces* **2016**, *8*, 7363−7369.
(82) Sahoo, G.; Polaki, S.R.; Ghosh, S.; Krishna, N.G.; Kamruddin, M. Temporal-stability of Plasma Functionalized Vertical Graphene Electrodes for Charge Storage. *J. Power Sources* **2018**, *401*, 37−48.
(83) Ghosh, S.; Sahoo, G.; Polaki, S. R.; Krishna, N. G.; Kamruddin, M.; Mathews, T. Enhanced Supercapacitance of Activated Vertical Graphene Nanosheets in Hybrid Electrolyte. *J. Appl. Phys.* **2017**, *122*, 214902.
(84) Ghosh, S.; Mathews, T.; Gupta, B.; Das, A.; Krishna, N. G.; Kamruddin, M. Supercapacitive Vertical Graphene Nanosheets in Aqueous Electrolytes. *Nano-Structures & Nano-Objects* **2017**, *10*, 42−50.
(85) Evlashin, S. A.; Maksimov, Y. M.; Dyakonov, P. V.; Pilevsky, A. A.; Maslakov, K. I.; Mankelevich, Y. A.; Voronina, E. N.; Vavilov, S. V.; Pavlov, A. A.; Zenova, E. V.; Akhatov, I. S.; Suetin, N. V. N-Doped Carbon NanoWalls for Power Sources. *Sci. Rep.* **2019**, *9*, 6716.
(86) Qi, J. L.; Wang, X.; Lin, J. H.; Zhang, F.; Feng, J. C.; Fei, W. D. Vertically Oriented Few-layer Graphene-nanocup Hybrid Structured Electrodes for High-performance Supercapacitors. *J. Mater. Chem. A* **2015**, *3*, 12396−12403.
(87) Quan, B. G.; Meng, Y. N.; Li, L.; Yao, Z. H.; Liu, Z.; Wang, K.; Wei, Z. X.; Gu, C. Z.; Li, J. J. Vertical few-layer graphene/metalized Si-nanocone arrays as 3D electrodes for solid-state supercapacitors with large areal capacitance and superior rate capability. *Appl. Surf. Sci.* **2017**, *404*, 238−245.
(88) Seo, D. H.; Yick, S.; Han, Z. J.; Fang, J. H.; Ostrikov, K. Synergistic Fusion of Vertical Graphene Nanosheets and Carbon Nanotubes for High-Performance Supercapacitor Electrodes. *ChemSusChem* **2014**, *7*, 2317−2324.
(89) Hsu, H. C.; Wang, C. H.; Nataraj, S. K.; Huang, H. C.; Du, H. Y.; Chang, S. T.; Chen, L. C.; Chen, K. H. Stand-up Structure of Graphene-like Carbon Nanowalls on CNT Directly Grown on Polyacrylonitrile-based Carbon Fiber Paper as Supercapacitor. *Diamond Relat. Mater.* **2012**, *25*, 176−179.
(90) Islam, N.; Warzywoda, J.; Fan, Z. Y. Edge-Oriented Graphene on Carbon Nanofiber for High-Frequency Supercapacitors. *Nano-Micro Lett.* **2018**, *10*, 9.
(91) Ma, Y.; Wang, M.; Kim, N.; Suhr, J.; Chae, H. A flexible Supercapacitor based on Vertically Oriented 'Graphene Forest' Electrodes. *J. Mater. Chem. A* **2015**, *3*, 21875−21881.
(92) Zhang, L.; DeArmond, D.; Alvarez, N. T.; Malik, R.; Oslin, N.; McConnell, C.; Adusei, P. K.; Hsieh, Y. Y.; Shanov, V. Flexible Micro-Supercapacitor Based on Graphene with 3D Structure. *Small* **2017**, *13*, 1603114.
(93) Shen, S. H.; Guo, W. H.; Xie, D.; Wang, Y. D.; Deng, S. J.; Zhong, Y.; Wang, X. L.; Xia, X. H.; Tu, J. P. A Synergistic Vertical Graphene Skeleton and S−C Shell to Construct High-performance $TiNb_2O_7$-based Core/shell Array. *J. Mater. Chem. A* **2018**, *6*, 20195−20204.
(94) Ouyang, B.; Zhang, Y. Q.; Zhang, Z.; Fan, H. J.; Rawat, R. S. Green Synthesis of Vertical Graphene Nanosheets and Their Application in High-performance Supercapacitors. *RSC Adv.* **2016**, *6*, 23968−23973.
(95) Ghosh, S.; Polaki, S. R.; Sahoo, G.; Jin, E. M.; Kamruddin, M.; Cho, J. S.; Jeong, S. M. Designing Metal Oxide-vertical Graphene Nanosheets Structures for 2.6 V Aqueous Asymmetric Electrochemical Capacitor. *J. Ind. Eng. Chem.* **2019**, *72*, 107−116.
(96) Han, Z. J.; Pineda, S.; Murdock, A. T.; Seo, D. H.; Ostrikov, K.; Bendavid, A. RuO_2-coated Vertical Graphene Hybrid Electrodes for High-performance Solid-state Supercapacitors. *J. Mater. Chem. A* **2017**, *5*, 17293−17301.
(97) Qi, H. L.; Yick, S.; Francis, O.; Murdock, A.; Van Der Laan, T.; Ostrikov, K.; Bo, Z.; Han, Z. J.; Bendavid, A. Nanohybrid TiN/Vertical Graphene for High-performance Supercapacitor Applications. *Energy Storage Mater.* **2020**, *26*, 138−146.
(98) Sahoo, G.; Polaki, S. R.; Krishna, N. G.; Kamruddin, M. Electrochemical Capacitor Performance of TiO_2 Decorated Vertical Graphene Nanosheets Electrode. *J. Phys. D: Appl. Phys.* **2019**, *52*, 375501.
(99) Zhao, C. M.; Wang, X.; Wang, S. M.; Wang, Y. Y.; Zhao, Y. X.; Zheng, W. T. Synthesis of $Co(OH)_2$/graphene/Ni Foam Nano-electrodes with Excellent Pseudocapacitive Behavior and High Cycling Stability for Supercapacitors. *Int. J. Hydrogen Energy* **2012**, *37*, 11846−11852.
(100) Liao, Q.; Li, N.; Jin, S.; Yang, G.; Wang, C. All-Solid-State Symmetric Supercapacitor Based on Co_3O_4 Nanoparticles on Vertically Aligned Graphene. *ACS Nano* **2015**, *9*, 5310−5317.
(101) Guerra, A.; Achour, A.; Vizireanu, S.; Dinescu, G.; Messaci, S.; Hadjersi, T.; Boukherroub, R.; Coffinier, Y.; Pireaux, J. J. ZnO/Carbon Nanowalls Shell/core Nanostructures as Electrodes for Supercapacitors. *Appl. Surf. Sci.* **2019**, *481*, 926−932.
(102) Dinh, T. M.; Achour, A.; Vizireanu, S.; Dinescu, G.; Nistor, L.; Armstrong, K.; Guay, D.; Pech, D. Hydrous RuO_2/carbon Nanowalls Hierarchical Structures for All-solid-state Ultrahigh-energy-density Micro-supercapacitors. *Nano Energy* **2014**, *10*, 288−294.
(103) Li, J. H.; Zhu, M. J.; Wang, Z. Q.; Ono, T. Engineering Micro-supercapacitors of Graphene Nanowalls/Ni Heterostructure Based on Microfabrication Technology. *Appl. Phys. Lett.* **2016**, *109*, 153901.
(104) Guo, W.; Yu, C.; Li, S. F.; Yang, J.; Liu, Z. B.; Zhao, C. T.; Huang, H. W.; Zhang, M. D.; Han, X. T.; Niu, Y. Y.; Qiu, J. S. High-Stacking-Density, Superior-Roughness LDH Bridged with Vertically Aligned Graphene for High-Performance Asymmetric Supercapacitors. *Small* **2017**, *13*, 1701288.
(105) Zhou, Y.; Cheng, X.; Huang, F.; Sha, Z.; Han, Z.; Chen, J.; Yang, W.; Yu, Y.; Zhang, J.; Peng, S.; Wu, S.; Rider, A.; Dai, L.; Wang, C. H. Hierarchically structured electrodes for moldable supercapacitors by synergistically hybridizing vertical graphene nanosheets and MnO2. *Carbon* **2021**, *172*, 272−282.
(106) Sha, Z.; Huang, F.; Zhou, Y.; Zhang, J.; Wu, S.; Chen, J.; Brown, S. A.; Peng, S.; Han, Z.; Wang, C. H. Synergies of vertical graphene and manganese dioxide in enhancing the energy density of carbon fibre-based structural supercapacitors. *Compos. Sci. Technol.* **2021**, *201*, 108568.

https://dx.doi.org/10.1021/acsami.0c19188
ACS Appl. Mater. Interfaces 2021, 13, 9561−9579

(107) Xiong, G. P.; Meng, C. Z.; Reifenberger, R. G.; Irazoqui, P. P.; Fisher, T. S. Graphitic Petal Electrodes for All-Solid-State Flexible Supercapacitors. *Adv. Energy Mater.* **2014**, *4*, 1300515.
(108) Shen, H. D.; Li, H. J.; Li, M. J.; Li, C. P.; Qian, L. R.; Su, L.; Yang, B. H. High-performance Aqueous Symmetric Supercapacitor Based on Polyaniline/vertical Graphene/Ti Multilayer Electrodes. *Electrochim. Acta* **2018**, *283*, 410−418.
(109) Zhang, H. H.; Tang, X. H.; Zhao, D. K.; Zheng, N.; Huang, L. B.; Sun, T. L.; Gu, C.; Ma, Y. G. Suppressing Charge Trapping Effect in Ambipolar Conducting Polymer with Vertically Standing Graphene as the Composite Electrode for High Performance Supercapacitor. *Energy Storage Mater.* **2020**, *29*, 281−286.
(110) Deng, S. J.; Chao, D. L.; Zhong, Y.; Zeng, Y. X.; Yao, Z. J.; Zhan, J. Y.; Wang, Y. D.; Wang, X. L.; Lu, X. H.; Xia, X. H.; Tu, J. P. Vertical graphene/$Ti_2Nb_{10}O_{29}$/hydrogen Molybdenum Bronze Composite Arrays for Enhanced Lithium Ion Storage. *Energy Storage Mater.* **2018**, *12*, 137−144.
(111) Ren, W. N.; Zhang, H. F.; Guan, C.; Cheng, C. W. Ultrathin MoS_2 Nanosheets@Metal Organic Framework-Derived N-Doped Carbon Nanowall Arrays as Sodium Ion Battery Anode with Superior Cycling Life and Rate Capability. *Adv. Funct. Mater.* **2017**, *27*, 1702116.
(112) Akbar, K.; Kim, J. H.; Lee, Z.; Kim, M.; Yi, Y.; Chun, S. H. Superaerophobic Graphene Nano-hills for Direct Hydrazine Fuel Cells. *NPG Asia Mater.* **2017**, *9*, e378.
(113) Feng, J.; Guo, Z. G. Wettability of Graphene: from Influencing Factors and Reversible Conversions to Potential Applications. *Nanoscale Horiz.* **2019**, *4*, 339−364.
(114) Roy, P. K.; Haider, G.; Chou, T. C.; Chen, K. H.; Chen, L. C.; Chen, Y. F.; Liang, C. T. Ultrasensitive Gas Sensors Based on Vertical Graphene Nanowalls/SiC/Si Heterostructure. *ACS Sens.* **2019**, *4*, 406−412.
(115) Yu, K. H.; Bo, Z.; Lu, G. H.; Mao, S.; Cui, S. M.; Zhu, Y. W.; Chen, X. Q.; Ruoff, R. S.; Chen, J. H. Growth of Carbon Nanowalls at Atmospheric Pressure for One-step Gas Sensor Fabrication. *Nanoscale Res. Lett.* **2011**, *6*, 202.
(116) Sobaszek, M.; Siuzdak, K.; Ryl, J.; Sawczak, M.; Gupta, S.; Carrizosa, S. B.; Ficek, M.; Dec, B.; Darowicki, K.; Bogdanowicz, R. Diamond Phase (sp^3-C) Rich Boron-Doped Carbon Nanowalls (sp^2-C): Physicochemical and Electrochemical Properties. *J. Phys. Chem. C* **2017**, *121*, 20821−20833.
(117) Teii, K.; Shimada, S.; Nakashima, M.; Chuang, A. T. H. Synthesis and electrical characterization of nn-type carbon nanowalls. *J. Appl. Phys.* **2009**, *106*, No. 084303.
(118) Zhang, Y.; Huang, C. J.; Duan, Z. H.; Liu, Q. F.; Wang, J. B.; Shi, W. Z. Enhanced Magnetoimpedance Effect of $Fe^{75.5}Cu^1Nb^3Si^{13.5}B^7$ Ribbon Covered by In-situ Growth Vertical Graphene Sheets. *Mater. Lett.* **2018**, *222*, 131−134.
(119) Wang, X. D.; Gao, D. L.; Li, M. J.; Li, H. J.; Li, C. P.; Wu, X. G.; Yang, B. H. CVD Graphene as an Electrochemical Sensing Platform for Simultaneous Detection of Biomolecules. *Sci. Rep.* **2017**, *7*, 7044.
(120) Tzouvadaki, I.; Aliakbarinodehi, N.; Pineda, D. D.; De Micheli, G.; Carrara, S. Graphene Nanowalls for High-performance Chemotherapeutic Drug Sensing and Anti-fouling Properties. *Sens. Actuators, B* **2018**, *262*, 395−403.
(121) Zheng, W.; Zhao, X. Electrochemical Stripping Analysis Using Vertically Free Standing Graphene containing Carbon Nanosheets as Electrode Materials. US patent, 20190376928A1, 2019.
(122) Lehmann, K.; Yurchenko, O.; Melke, J.; Fischer, A.; Urban, G. High Electrocatalytic Activity of Metal-free and Non-doped Hierarchical Carbon Nanowalls Towards Oxygen Reduction Reaction. *Electrochim. Acta* **2018**, *269*, 657−667.
(123) Evlashin, S.; Svyakhovskiy, S.; Suetin, N.; Pilevsky, A.; Murzina, T.; Novikova, N.; Stepanov, A.; Egorov, A.; Rakhimov, A. *Carbon* **2014**, *70*, 111.
(124) Wang, Y.; Li, J.; Song, K. Study on Formation and Photoluminescence of Carbon Nanowalls Grown on Silicon Substrates by Hot Filament Chemical Vapor Deposition. *J. Lumin.* **2014**, *149*, 258−263.
(125) Wang, B. B.; Zhu, K.; Ostrikov, K.; Shao, R. W.; Zheng, K. Structure and Photoluminescence Properties of Carbon Nanotip-vertical Graphene Nanohybrids. *J. Appl. Phys.* **2016**, *119*, No. 024302.
(126) Roy, P. K.; Haider, G.; Lin, H.; Liao, Y. M.; Lu, C. H.; Chen, K. H.; Chen, L. C.; Shih, W. H.; Liang, C. T.; Chen, Y. F. Multicolor Ultralow-Threshold Random Laser Assisted by Vertical-Graphene Network. *Adv. Opt. Mater.* **2018**, *6*, 1800382.
(127) Zhu, L.; Huang, Y.; Yao, Z.; Quan, B.; Zhang, L.; Li, J.; Gu, C.; Xu, X.; Ren, Z. Enhanced Polarization-sensitive Terahertz Emission from Vertically Grown Graphene by a Dynamical Photon Drag Effect. *Nanoscale* **2017**, *9*, 10301−10311.
(128) Ci, H. N.; Ren, H. Y.; Qi, Y.; Chen, X. D.; Chen, Z. L.; Zhang, J. C.; Zhang, Y. F.; Liu, Z. F. 6-in. Uniform Vertically-oriented Graphene on Soda-lime Glass for Photothermal Applications. *Nano Res.* **2018**, *11*, 3106−3115.
(129) Zheng, W.; Zhong, X. Z.; Chen, W. S.; Shi, L. T.; Zhao, X. An Optical Heating Film Made by Vertical Graphene. Patent CN 210899675 U, 2019.
(130) Zhang, P. P.; Li, J.; Lv, L. X.; Zhao, Y.; Qu, L. T. Vertically Aligned Graphene Sheets Membrane for Highly Efficient Solar Thermal Generation of Clean Water. *ACS Nano* **2017**, *11*, 5087−5093.
(131) Zhang, Y. F.; Ren, Y. J.; Bai, S. L. Vertically Aligned Graphene Film/epoxy Composites as Heat Dissipating Materials. *Int. J. Heat Mass Transfer* **2018**, *118*, 510−517.
(132) Ma, Y. F.; Jang, H.; Kim, S. J.; Pang, C.; Chae, H. Copper-Assisted Direct Growth of Vertical Graphene Nanosheets on Glass Substrates by Low-Temperature Plasma-Enhanced Chemical Vapour Deposition Process. *Nanoscale Res. Lett.* **2015**, *10*, 308.

https://dx.doi.org/10.1021/acsami.0c19188
ACS Appl. Mater. Interfaces 2021, 13, 9561−9579